Journal of Medicinal Chemistry

pubs.acs.org/jmc

Article

Ketoprofen and Loxoprofen Platinum(IV) Complexes Displaying Antimetastatic Activities by Inducing DNA Damage, Inflammation Suppression, and Enhanced Immune Response

Zuojie Li, Qingpeng Wang,* Linming Li, Yan Chen, Jichun Cui, Min Liu, Ning Zhang,* Zhifang Liu,* Jun Han, and Zhengping Wang

Cite This: *J. Med. Chem.* 2021, 64, 17920−17935

Read Online

ACCESS | Metrics & More | Article Recommendations | Supporting Information

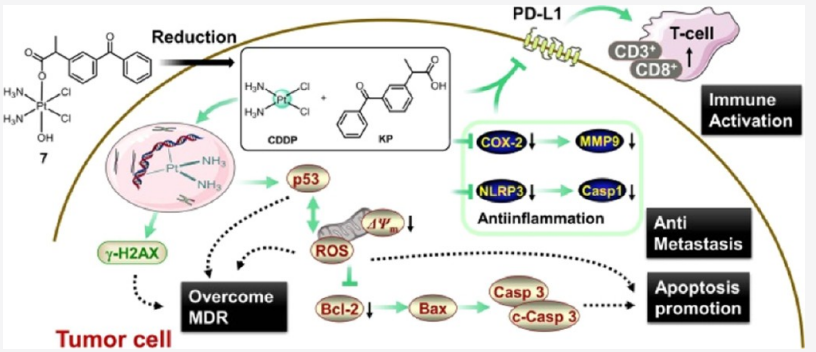

ABSTRACT: Metastasis is a major contributor of death in cancer patients, and there is an urgent need for effective treatments of metastatic malignancies. Herein, ketoprofen (KP) and loxoprofen (LP) platinum(IV) complexes with antiproliferative and antimetastatic properties were designed and prepared by integrating chemotherapy and immunotherapy targeting cyclooxygenase-2 (COX-2), matrix metalloproteinase-9 (MMP-9), and programmed death ligand 1 (PD-L1), besides DNA. A mono-KP platinum(IV) complex with a cisplatin core is screened out as a candidate possessing potent anti-proliferative and anti-metastasis activities both in vitro and in vivo. It induces serious DNA damage and further leads to high expression of γ-H2AX and p53. Moreover, it promotes apoptosis of tumor cells through mitochondrial apoptotic pathway Bcl-2/Bax/caspase3. Then, COX-2, MMP-9, NLRP3, and caspase1 as pivotal enzymes igniting inflammation and metastasis are obviously inhibited. Notably, it significantly improves immune response through restraining the expression of PD-L1 to increase $CD3^+$ and $CD8^+$ T infiltrating cells in tumor tissues.

INTRODUCTION

Cancer is a leading cause of death worldwide, and metastasis contributes to approximately 90% of mortality for patients suffering from cancer,[1,2] whereas traditional anticancer agents have weak curative effects on metastatic cancers. Drugs with special and effective antimetastatic properties are highly desired in clinic.[3] Therefore, the development of novel antimetastatic agents has become a great challenge for scientists in medicinal and pharmaceutical fields.

Platinum drugs as a chemotherapeutical arsenal represent a major breakthrough in cancer treatment. Especially, cisplatin (CDDP), carboplatin (CBP), and oxaliplatin (OLP) (Figure 1) show appealing antitumor activities by forming intrastrand DNA cross-links for treatment of various neoplasms including lung, testicular, ovarian, cervical, head, neck, and colorectal cancers and so forth.[4−6] Nevertheless, their therapeutic outcomes are rather plagued with severe toxicity and the development of resistance. Additionally, their roles in treating metastatic cancer are extremely limited in clinic.

Platinum(IV) complexes supply an effective way to develop various novel platinum agents with multitargeting antitumor mechanisms by the incorporation of desired functional groups at the axial positions.[7−9] Moreover, as prodrugs of platinum(II) complexes, platinum(IV) hybrids possess many fascinating advantages over their precursors and are of great potential to be developed as the next generation of platinum drugs.[10,11] The platinum(IV) complex with a d^2sp^3 octahedral configuration is more substitution-inert in normal biological media than the labile platinum(II) drugs, which enables the platinum(IV) compound to undergo fewer reducing side effects and off-target reactions and further reduce toxicities.

Received: July 11, 2021
Published: December 1, 2021

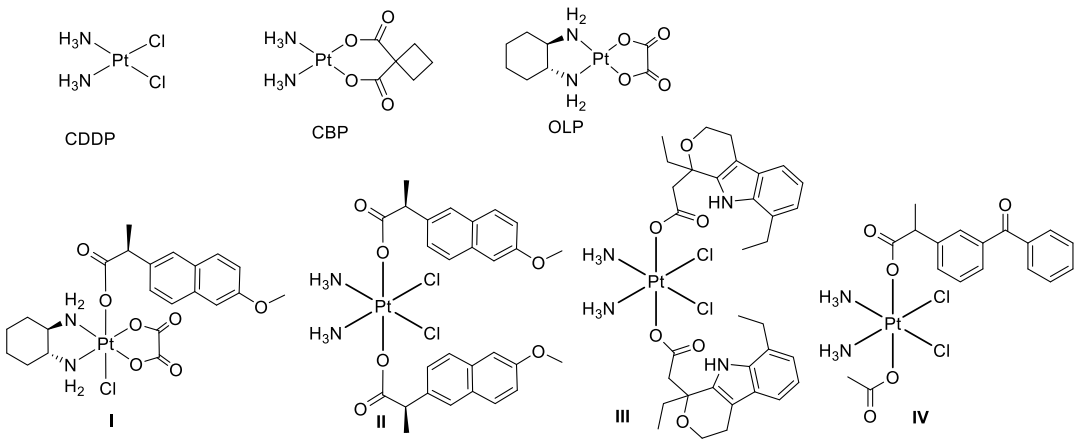

Figure 1. Structures of platinum(II) drugs CDDP, CBP, and OLP and platinum(IV) complexes **I**–**IV**.

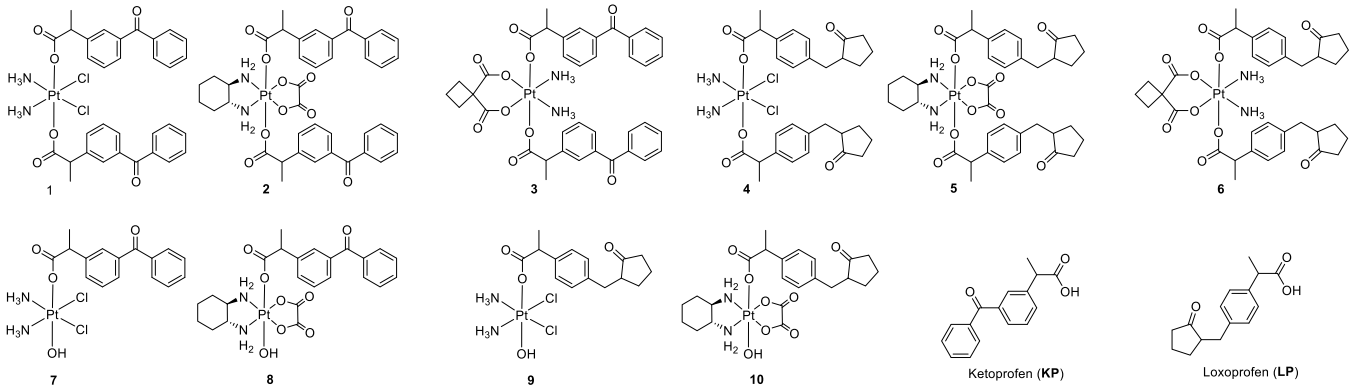

Figure 2. Structures of platinum(IV) complexes **1**–**10** and KP and LP.

Besides, the activation of platinum(IV) complexes via the reduction by ascorbic acid (AsA) and GSH happens more likely in the reducing tumor microenvironment (TME), which would be in favor of enhancing tumor selectivity. Thereby, the development of novel effective platinum(IV) drugs has attracted extensive attention in the past decade.

Cancer-related inflammation as a hallmark of cancer has become an encouraging target for cancer therapy.[12] Numerous pieces of evidence suggest that dysregulated inflammatory response significantly promotes the formation of TME and plays a pivotal role in sustaining immunosuppression, tumor cell proliferation, extracellular matrix breakdown, metastasis, and drug resistance.[13,14] Thus, the development of novel anticancer drugs with inflammatory inhibition competence appears to be an attracting strategy for the exploration of effective chemotherapeutics with durable antitumor responses. Cyclooxygenase-2 (COX-2) as the primary target for inflammation inhibition is overexpressed in various cancers such as colonic, lung, prostate, gastrointestinal, and cervical cancers.[15] Furthermore, the overexpression of COX-2 would promote the expression of matrix metalloproteinases (MMPs) in tumor tissues, which could degrade the basement membrane and markedly boost metastasis and inflammation.[16,17] Enzymes COX-2 and MMPs are promising targets for attenuating cancer-related inflammation and metastasis.

Immune suppression is another hallmark of cancer which could facilitate cancer cells evading from immunosurveillance in TME.[12,18] Compromised antitumor immunity is capable of accelerating tumor-recruited inflammation and metastases. Integration of chemotherapy and immunotherapy paves a new way for the treatment of metastatic tumors. Programmed death ligand 1 (PD-L1) overexpressed in various cancers displays major roles in alleviating immunity by suppressing activated T lymphocytes.[19−21] Recently, it was established that selective inhibition of COX-2 provides a novel approach to regulate PD-L1 expression in cancers and further stimulate antitumor immune response.[17,22,23] Collectively, PD-L1 as one of the most important immunology checkpoints for immune therapies is a promising target for immune activation, inflammation reduction, and blocking cancer metastases.

The investigation on platinum(IV) complexes possessing simultaneous antiproliferative and antimetastatic activities is an important topic in platinum drug exploration. Great efforts have been devoted to develop novel structural platinum(IV) complexes with NSAID ligands as antitumor agents.[24−34] Recently, several NSAID platinum(IV) complexes **I**–**III** (Figure 1) with naproxen and etodolac ligands were proven effective in inhibiting metastasis of tumor cells in vitro by suppressing the expression of COXs, which indicated the great potential of NSAID platinum(IV) complexes as antimetastatic agents.[25,27,28] Ketoprofen (KP) and loxoprofen (LP) as important NSAIDs with potent anti-inflammatory activities are of great potential to be used as antitumor agents with antimetastatic properties. KP could effectively inhibit the expression of matrix metalloproteinases and vascular endothelial growth factor in osteosarcoma, thus displaying suppression of tumor growth and metastasis.[35,36] Meanwhile, LP was effective in inhibiting tumor growth in vivo by reducing

https://doi.org/10.1021/acs.jmedchem.1c01236
J. Med. Chem. 2021, 64, 17920−17935

Scheme 1. Synthetic Route of Platinum(IV) Complexes 1−10

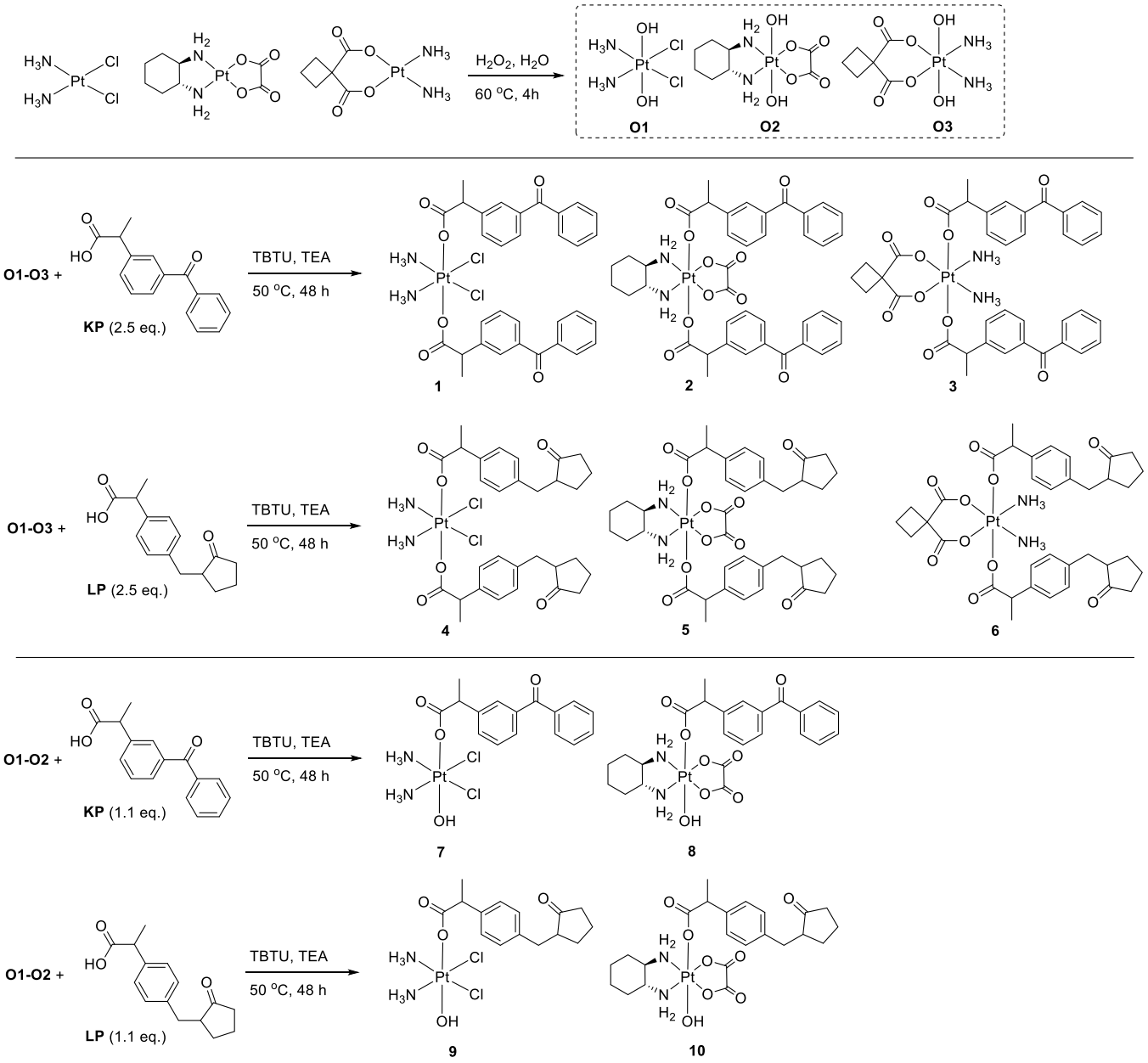

intratumoral vessel density.[37] Recently, a CDDP-based platinum(IV) combo **IV** (Figure 1) with the KP ligand was reported to suppress the proliferation of a panel of human tumor cell lines effectively and could inhibit metastasis of MDA-MB-231 cells in vitro by restraining epithelial-to-mesenchymal transition.[38,39] Subsequently, their antimetastasis performance in vivo and action mechanisms are deserved for further detection. Inspired by these conditions and as a continuation of our interest in developing new antimetastatic platinum(IV) drugs,[40−42] herein KP and LP platinum(IV) hybrids **1−10** (Figure 2) were designed with the aim of developing a series of new platinum complexes with chemotherapeutic and immunotherapeutic effects targeting COXs, MMPs, and PD-L1. Their antitumor and antimetastatic activities were evaluated in vitro and in vivo, and the mechanisms in causing DNA lesion, suppressing tumor-recruited inflammation, and modulating immunity were investigated.

RESULTS AND DISCUSSION

Chemistry. The syntheses of platinum(IV) complexes **1−10** with KP and LP ligands were started from the oxidation of CDDP, OLP, and CBP with hydrogen peroxide according to the published procedures[40−42] (Scheme 1), which afforded the corresponding oxoplatins **O1−O3** with double hydroxyl axial ligands. Dual-substituted platinum(IV) complexes **1−6** were prepared by the condensation of oxoplatins **O1−O3** with 2.5 equivalents of KP or LP in the presence of *N,N,N′,N′*-tetramethyl-*O*-(benzotriazol-1-yl)uronium tetrafluoroborate (TBTU) and *N,N,N*-triethylamine (TEA) in yields of 21.7−31.0%. Meanwhile, the conjunction of oxoplatins **O1−O2** with 1.1 equivalents of KP or LP afforded monosubstituted platinum(IV) complexes **7−10** in yields of 23.4−33.5%.

https://doi.org/10.1021/acs.jmedchem.1c01236
J. Med. Chem. 2021, 64, 17920−17935

Table 1. Antiproliferative Activities of Platinum(IV) Complexes 1−10 toward Six Carcinoma Cell Lines and One Normal Cell Line[a]

compounds.	SKOV-3	A549	A549R	RF[b]	4T1	CT-26	HepG2	LO2	SI[c]
1	0.079 ± 0.017	0.49 ± 0.10	0.18 ± 0.04	0.37	0.35 ± 0.01	2.31 ± 0.02	0.18 ± 0.03	0.51 ± 0.06	2.81
2	0.86 ± 0.25	5.49 ± 0.34	10.22 ± 3.41	1.86	31.08 ± 5.35	19.79 ± 2.12	11.27 ± 2.05	7.41 ± 2.32	0.66
3	18.94 ± 2.65	37.58 ± 6.36	61.07 ± 3.31	1.63	38.27 ± 5.08	40.19 ± 2.54	14.88 ± 3.12	29.46 ± 1.68	1.98
4	0.086 ± 0.012	0.65 ± 0.13	0.43 ± 0.06	0.66	0.85 ± 0.13	6.28 ± 0.56	0.56 ± 0.19	0.70 ± 0.19	1.24
5	10.34 ± 2.51	34.87 ± 8.39	24.28 ± 3.26	0.70	48.50 ± 5.08	32.53 ± 4.35	12.48 ± 1.18	21.72 ± 3.06	1.74
6	32.64 ± 5.71	>50	>50	ND[d]	ND	ND	>50	ND	ND
7	0.33 ± 0.08	1.99 ± 0.26	1.45 ± 0.47	0.73	2.25 ± 0.34	2.09 ± 0.28	0.44 ± 0.09	1.45 ± 0.11	3.33
8	4.05 ± 1.64	25.27 ± 5.83	13.50 ± 5.57	0.53	16.14 ± 1.74	19.10 ± 3.80	4.90 ± 0.36	28.34 ± 1.36	5.78
9	1.54 ± 0.28	4.66 ± 0.76	13.56 ± 2.25	2.91	20.33 ± 1.30	7.68 ± 1.54	1.59 ± 0.37	7.41 ± 0.49	4.66
10	15.62 ± 4.48	32.78 ± 5.87	18.48 ± 2.89	0.56	34.10 ± 0.39	60.49 ± 5.29	29.96 ± 6.86	41.27 ± 3.67	1.38
KP	>50	>50	>50	ND	ND	ND	ND	ND	ND
LP	>50	>50	>50	ND	ND	ND	ND	ND	ND
CDDP + KP (1:1)[e]	1.42 ± 0.21	3.55 ± 0.69	9.24 ± 1.85	2.60	6.43 ± 1.12	2.86 ± 0.17	2.10 ± 0.16	2.53 ± 0.28	1.20
OLP + KP (1:1)[e]	1.08 ± 0.16	7.36 ± 1.68	7.95 ± 2.03	1.08	8.46 ± 1.82	6.28 ± 0.47	5.72 ± 0.68	2.97 ± 0.43	0.52
CDDP	0.71 ± 0.05	5.18 ± 0.45	16.05 ± 2.40	3.10	4.62 ± 0.95	1.84 ± 0.28	3.26 ± 0.45	2.78 ± 0.10	0.85
OLP	0.66 ± 0.14	9.68 ± 1.72	9.63 ± 0.43	0.99	13.29 ± 4.42	4.70 ± 0.41	4.71 ± 0.32	3.72 ± 0.24	0.79
CBP	29.90 ± 1.30	>50	48.64 ± 6.98	ND	>50	>50	ND	>50	ND

[a]The IC_{50} (μM) values were calculated for 48 h continuous drug treatment based on three parallel experiments. [b]RF: resistant factor, RF = IC_{50}(A549R)/IC_{50}(A549). [c]SI: selectivity index, SI = IC_{50}(LO2)/IC_{50}(HepG2). [d]ND: not tested or not calculated. [e]CDDP/OLP + KP (1:1): mixture of CDDP/OLP and KP with a molar ratio of 1:1.

Antitumor Activities In Vitro. The antiproliferative activities of platinum(IV) complexes **1**−**10** with KP and LP ligands were determined with CDDP, OLP, CBP, KP, and LP as reference drugs using a 3-(4,5-dimethylthiazol-2-yl)-2,5-diphenyltetrazolium bromide (MTT) assay. The mixtures of CDDP and OLP with KP (CDDP/OLP + KP, 1:1) were also tested. Six tumor cell lines including human ovarian cancer (SKOV-3), human lung cancer (A549), CDDP-resistant human lung cancer (A549R), murine breast cancer (4T1), murine colon cancer (CT-26), human liver cancer (HepG2), and one human normal liver cell line (LO2) were evaluated. The results were given as IC_{50} values in Table 1 based on three parallel experiments. To detect the influence of incubation time on the activities, the IC_{50} values of platinum complexes **1** and **7**, CDDP, and OLP against CT26 were evaluated for 24, 48 , and 72 h continuous treatments (Table S1). It is disclosed that the tested platinum complexes especially platinum(IV) complexes **1** and **7** display relatively lower activities after 24 h treatment, and the IC_{50} values decrease at 48 h, and the activities at 72 h are similar to that of 48 h. Thus, the antitumor activities after 48 h continuous treatment were tested in this work.

It is realized that the combined administration of CDDP and OLP with KP (CDDP/OLP + KP, 1:1) leads to weak impacts on the antitumor activities in comparison with CDDP and OLP, which is mainly in accordance with the literature.[27,31,43] Meanwhile, the platinum(IV) complexes with CDDP, OLP, and CBP cores display rather different performances with the corresponding platinum(II) drugs. The platinum core has significant impacts on antitumor activities of these platinum-(IV) complexes in a sequence: CDDP > OLP > CBP. Platinum(IV) complexes **1**, **4**, **7**, and **9** with a CDDP core display prominent antitumor activities against all the tested tumor cell lines. Especially, complexes **1**, **4**, and **7** afford lower IC_{50} values of SKOV-3, A549, A549R, 4T1, and HepG2 than the corresponding platinum(II) reference drug CDDP. The KP-modified platinum(IV) compounds **1** and **7** are relatively more effective than the corresponding LP-derived ones **4** and **9**. Moreover, it is noticed that compounds **1** and **4** with dual ligands display superior activities compared with the monoligand ones **7** and **9** in vitro. Especially, against SKOV-3, A549, A549R, 4T1, and HepG2, hybrids **1** and **4** afford low IC_{50} values in the nM grade (0.08−0.85 μM), which are over 5.4−89.2 times lower than CDDP, OXP, and CBP. Meanwhile, complex **7** also exerts effective inhibitory efficacy toward SKOV-3, A549, A549R, and HepG2 cells with IC_{50} values ≤1.99 μM, which are more efficient than the platinum(II) drugs.

To judge the potency of the title compounds in defeating drug resistance of CDDP, the resistant factor (RF) as a ratio of the IC_{50} value of A549R to that of A549 was calculated. Potent complexes **1**, **4**, and **7** also possess great potential in overcoming drug resistance leading to low RF values (0.37, 0.66, and 0.73), which are over 4.2 times lower than CDDP (RF = 3.10). However, compound **9** with a mono-LP ligand affords a high RF value of 2.91. Subsequently, the selectivity index (SI) defined as a ratio of IC_{50} for normal liver cell LO2 to that of liver tumor cell HepG2 was calculated to determine the tumor selective potential of the tested complexes. KP-derived platinum(IV) complexes **1** and **7** give high SI values of 2.81 and 3.33, which are superior to CDDP and OLP (SI = 0.85 and 0.79). Meanwhile, the mixtures of CDDP and OLP with KP (CDDP/OLP + KP) exert no significant positive influence on improving RF and SI values.

Accordingly, the incorporation of KP and LP ligands into a platinum(IV) system exerts much positive influence on overcoming the resistance of CDDP and improving tumor selective competence, which are superior to that of the mixtures CDDP/OLP + KP. Especially, complexes **1**, **4**, **7**, and **9** with a cisplatin core displaying promising antitumor activities in vitro are worthy for further investigation as antitumor agents in vivo.

Antitumor Activities In Vivo. To detect the antitumor potency of KP and LP platinum(IV) complexes in vivo, the

https://doi.org/10.1021/acs.jmedchem.1c01236
J. Med. Chem. 2021, 64, 17920−17935

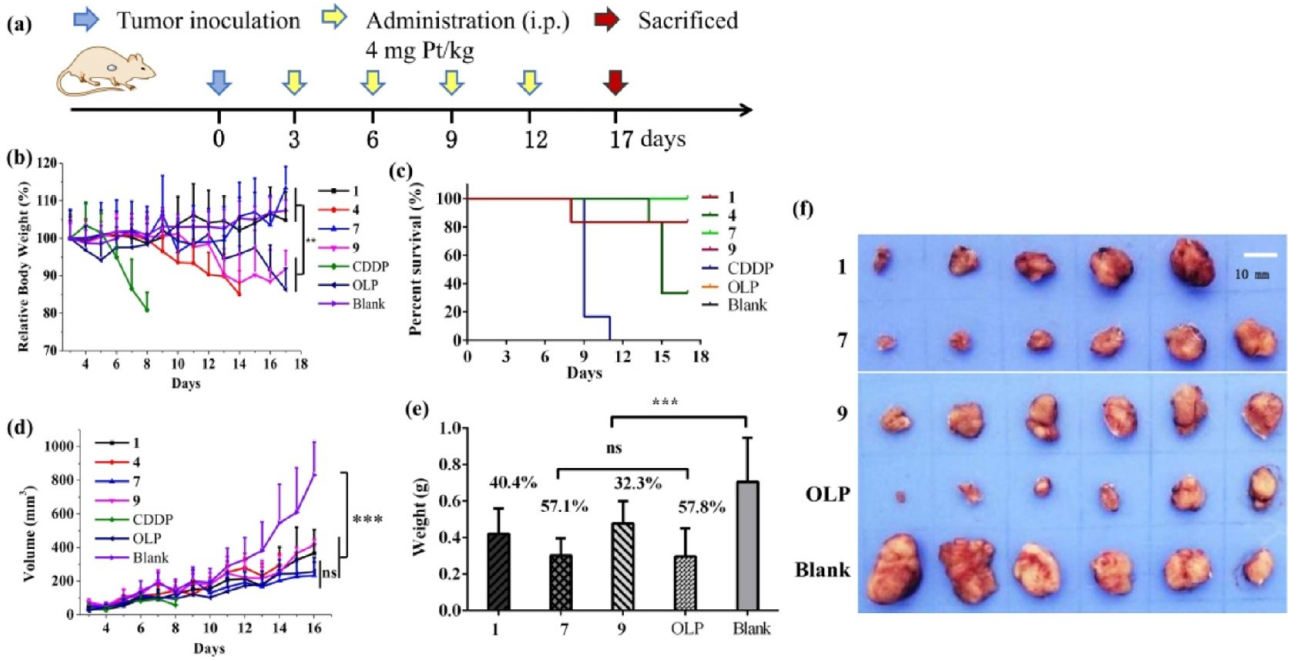

Figure 3. In vivo antitumor activities of compounds **1**, **4**, **7**, and **9**, CDDP, and OLP to CT-26 tumors in BALB/c mice ($n = 6$). $^{*}P < 0.05$, $^{**}P < 0.01$, $^{***}P < 0.001$, and *ns*: no significant difference. (a) Schematic illustration of the experimental design. (b) Relative body weight of the mice during the treatment. (c) Survival analysis of mice during the treatment. (d) Tumor growth as a function of time. (e) Tumor weight of each group at the end of the experiment. The tumor growth inhibition (TGI) of the tested drugs in comparison with the saline group is depicted above the column (TGI = (1 − tumor weight of the drug-treated group/tumor weight of the saline group) × 100%). (f) Image of tumors on day 17 after the mice sacrificed.

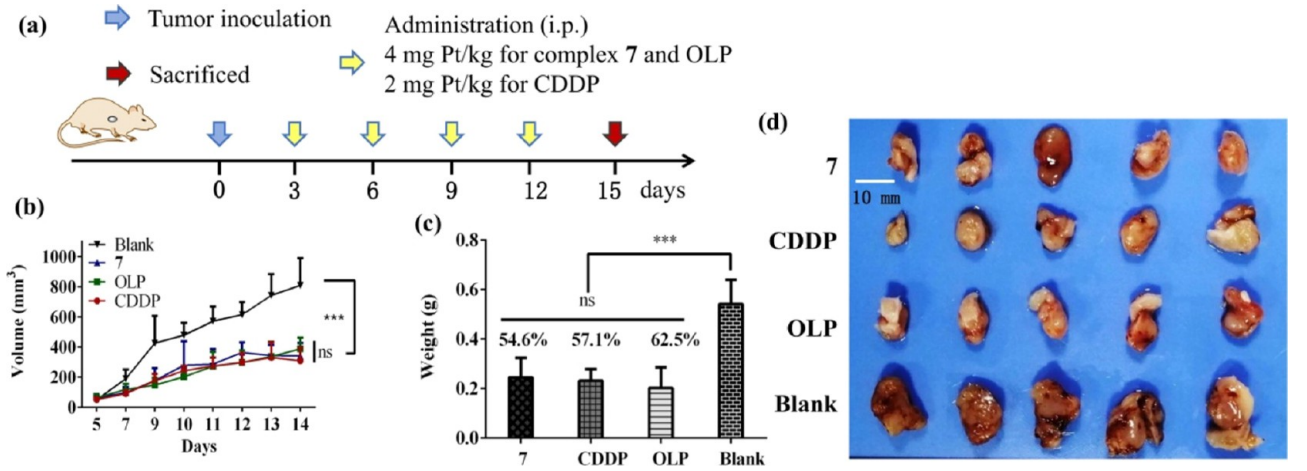

Figure 4. In vivo antitumor activities of compound **7**, CDDP, and OLP to 4T1 tumors in BALB/c mice ($n = 5$). $^{*}P < 0.05$, $^{**}P < 0.01$, $^{***}P < 0.001$, and *ns*: no significant difference. (a) Schematic illustration of the experimental design. (b) Tumor growth as a function of time. (c) Tumor weight in each group at the end of the experiment. The TGI is depicted above the column. (d) Image of tumors on day 15 after the mice were sacrificed.

activities of complexes **1**, **4**, **7**, and **9** were evaluated on male BALB/c mice bearing CT-26 homograft tumors. The drugs were administered at the same dosage of 4 mg Pt kg^{-1} (i.p.) four times on days 3, 6, 9, and 12 using CDDP and OLP as reference drugs, and the saline group was set as the blank (Figure 3a).

The body weight and survival rate of the mice during the treatment as important indexes to evaluate the systemic toxicity of drugs are drawn in Figure 3b,c. It is realized that CDDP caused rapid loss of body weight of 19.2% in 5 days after two administrations (day 8). Then, massive death of mice was induced by CDDP on day 9 to decrease the survival rate to 16%, which indicated its serious toxic influence onto mice. Then, complex **4** with dual LP ligands also exerted obvious toxicity that it caused a remarkable body weight loss of 14.9% on day 14. Then, its survival rate decreased to 33% on day 15. Therefore, complex **4** and CDDP were not further analyzed taking their toxicity in consideration. No decrease in the survival rate was observed in complexes **7** and **9** and OLP groups; meanwhile, one mouse died in the complex **1**-treated group on day 8. Moreover, complex **7** exerted no visible impacts on body weight of mice in comparison with the blank group (P = ns), which was obviously superior to reference drug OLP ($P < 0.01$) and complex **9** ($P < 0.01$), indicating its low

https://doi.org/10.1021/acs.jmedchem.1c01236
J. Med. Chem. 2021, 64, 17920−17935

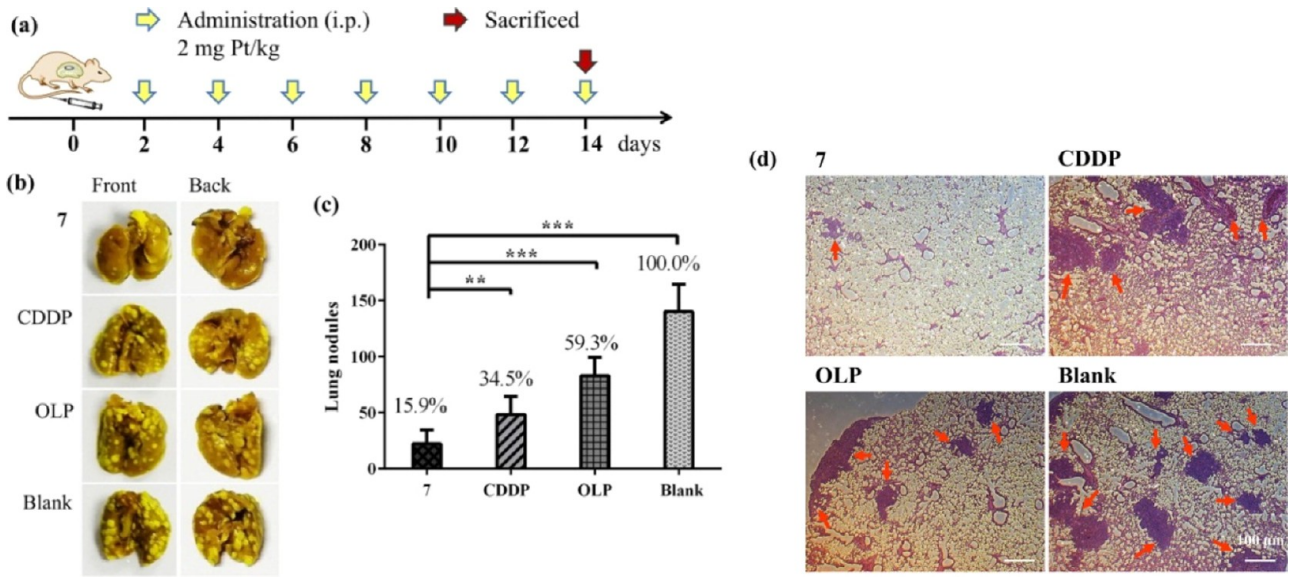

Figure 5. Pulmonary metastasis inhibition of compound 7, CDDP, and OLP against 4T1 breast carcinoma tumors in vivo ($n = 5$). *$P < 0.05$, **$P < 0.01$, ***$P < 0.001$, and *ns*: no significant difference. (a) Schematic illustration of the experimental design. (b) Representative photographs of pulmonary metastasis from each group on day 14 after the mice were sacrificed. (c) Lung nodules in each group. (d) H&E staining of lung metastasis nodules. Nodules were signed with red arrows.

toxicity in vivo. Additionally, the hematoxylin and eosin (H&E) staining of liver, spleen, and kidney slices discloses that no significant appreciable histological differences are observed in the slices of the 7-treated groups in comparison with the saline group (Figure S2).

Tumor volume was monitored along the experiment (Figure 3d). All tumors were harvested from mice on day 17 after the mice were sacrificed. The TGI rate (TGI = (1 − tumor weight of the drug-treated group/tumor weight of the saline group) × 100%) was calculated (Figure 3e,f). Complex **7** with a mono-KP ligands exhibits the most effective suppression to tumor growth in vivo (232 mm^3) with TGI = 57.1% in contrast to the saline group (830 mm^3, $P < 0.001$), which is comparable to that of OLP (256 mm^3, TGI = 57.8%, P = ns). Notably, the antitumor competence of compound **7** is more potent than complex **1** with dual KP ligands (365 mm^3, TGI = 40.4%). The trend of results in vivo in this work is rather distinct from that in vitro. The H&E staining of tumor slices in Figure S3 indicates that severe degeneration/necrosis with the dispersion of nucleus is observed in the **1**-, 7-, and **9**-treated slices, which is similar to that of OLP, indicating the apoptosis of tumor cells.

In order to further verify whether complex **7** is effective toward different tumors, its potency against 4T1 homograft tumors on female BALB/c mice in vivo was also tested. Complex **7** and OLP were administered at a dosage of 4 mg Pt kg^{-1} on days 3, 6, 9, and 12 with saline as the blank group, while the dosage of CDDP was decreased to 2 mg Pt kg^{-1} taking its toxicity in consideration. The results in Figure 4 reflect that complex **7** also exhibits prominent tumor growth inhibition to 4T1 tumors with a TGI of 54.6%, which is similar to that of the CT-26 tumor results.

Accordingly, platinum(IV) complex **7** with a mono-KP ligand possesses the most promising antitumor performance with high antitumor efficacy and low toxicity in vivo and is investigated as a candidate for antimetastatic activities.

Metastasis Inhibition In Vitro and In Vivo. Encouraged by the prominent antitumor effects of complex **7** in vitro and in vivo, we extended its application into inhibiting metastasis of aggressive tumors. Lung is a major site of extrahepatic metastasis. Herein, pulmonary metastasis models were established by injection of 4T1 cells (2×10^5 cells) via the tail vein. Complex **7**, CDDP, and OLP were administered at a dosage of 2 mg Pt/kg (i.p.) seven times at 2 day interval with saline as the blank (Figure 5). Complex **7** leads to a small amount of pulmonary metastasis nodules (15.9%) in contrast to the blank group, which is significantly superior to CDDP (34.5, $P < 0.01$) and OLP (59.3%, $P < 0.001$). Furthermore, the size of metastatic nodules examined by H&E staining in the lung from the complex 7-treated group is obviously smaller than that from the blank group as well as CDDP and OLP groups (Figure 5d). These facts indicate that complex **7** displays significantly more effective antimetastasis effects than CDDP and OLP in vivo.

Then, the tumor metastasis inhibitory properties of compound **7** in vitro were also testified by wound-healing and transwell assays. Results of wound-healing assay (Figure 6) demonstrate that complex **7** (10 μM) is more effective in reducing healing of 4T1 cells with a lower wound-healing rate of 23.5% than CDDP (43.6%) and OLP (67.5%). Then, the transwell experiment (Figure 7) further evidences the powerful potency of complex **7** in attenuating metastasis of tumor cells.

Summarily, the abovementioned results disclose that a candidate complex **7** with pronounced metastasis inhibitory properties both in vitro and in vivo is screened out in this work and is of great potential for further investigation as a novel antimetastatic drug. The action mechanism was detected in the following experiments.

Drug Accumulation in Tumor Cells In Vitro and In Vivo. The drug accumulation in tumor cells is a key index influencing antitumor competence and tumor-targeting properties of platinum chemotherapeutics. Proper lipid−water partition is an important factor influencing the drug accumulation and further affecting antitumor activities.[38,44] The lipid−water partition coefficient (Log $P_{o/w}$) of complexes **1** and **7** was tested. The drug accumulations in tumor cells and

https://doi.org/10.1021/acs.jmedchem.1c01236
J. Med. Chem. 2021, 64, 17920−17935

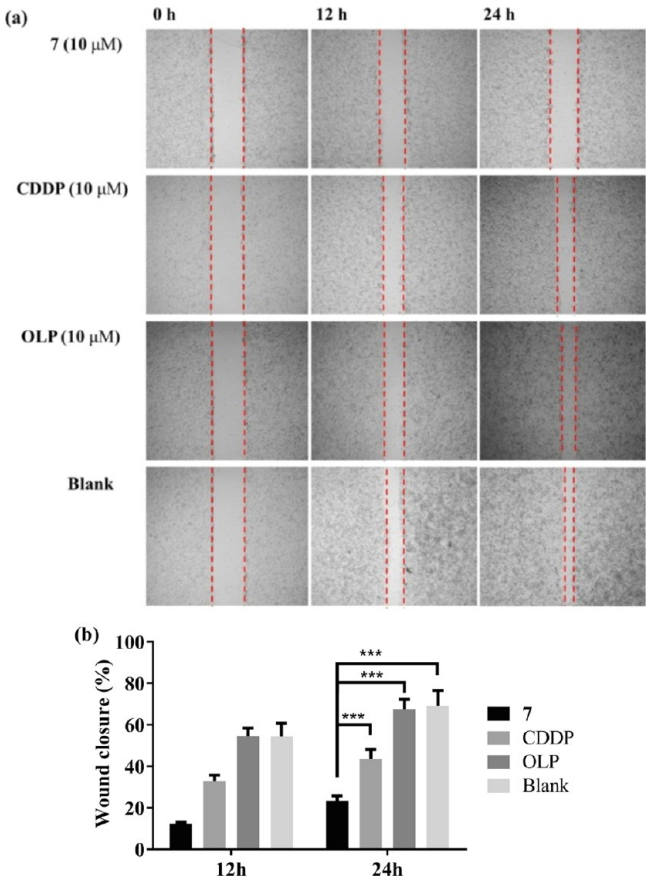

Figure 6. Migration inhibition to 4T1 cells of complex 7, CDDP, and OLP at 10 μM in vitro. The extent of wound healing was observed at 0, 12, and 24 h. (a) Representative images. (b) Analysis of wound closure. *P < 0.05, **P < 0.01, ***P < 0.001, and *ns*: no significant difference.

DNA in vitro were determined with ICP−MS after CT-26 cells were treated with compounds **1** and **7**, CDDP, and OLP (10 μM) for 24 h at 37 °C. In addition, the platination level in CT-26 tumor tissues in vivo was also measured. Results in Figure 8 reflect that complexes **1** and **7** possess different accumulation trends in vitro and in vivo that complex **1** accumulates higher in tumor cells than compound **7** in vitro; meanwhile, complex **7** leads to more platination in tumor tissues in vivo. The accumulation level of platinum(IV) drugs in tumor cells in vitro is positively correlated with lipophilicity that dual KP platinum(IV) complex **1** with higher Log $P_{o/w}$ = 2.47 ± 0.13 (Table S2) leads to a higher platinated level in whole cells than mono-KP complex **7** (Log $P_{o/w}$ = 0.79 ± 0.03) as well as platinum(II) drugs CDDP (Log $P_{o/w}$ = −2.30)[45] and OLP (Log $P_{o/w}$ = −1.54).[45] Then, drug accumulation in DNA is also increased for compound **1** in comparison with complex **7**, CDDP, and OLP. Meanwhile, the platination level in CT-26 tumor tissues in vivo reveals that mono-KP platinum(IV) complex **7** accounts for 7.7-fold higher platinum accumulation (4.6 μg/g) than that of complex **1** (0.6 μg/g) with dual KP ligands, which are mainly consistent with their antitumor activities in vivo. Furthermore, complex **7** also leads to significantly enhanced drug accumulation in tumor tissues in contrast to OLP (1.2 μg/g). Taking the promising stability (Figure S11a) and high uptake of candidate complex **7** in consideration, it could be assumed that complex **7** enters tumor cells as an intact lipophilic molecule and exerts a distinct antitumor mechanism with its precursor CDDP.[46] Drug accumulation in tumor cells seems a pivotal factor affecting antitumor activities of KP platinum(IV) hybrids both in vitro and in vivo.

Reduction and DNA Damage Properties. As a prodrug of platinum(II) drugs, platinum(IV) complexes show antitumor activities by causing DNA damage after reduction to platinum(II) compounds. Thereby, the reduction potential and DNA-binding properties of candidate complex **7** were testified by the HPLC method in phosphate-buffered saline (PBS) and biological media RPMI1640[47] in the absence and presence of bioreductant AsA. Complex **7** mainly keeps stable in PBS and RPMI1640 for at least 24 h at 37 °C (Figures S7 and S11a). Then, it undergoes easily reduction to platinum(II) form in the presence of AsA (1 mM, similar concentration as in TME) (Figures S8 and S11a) with the release of KP. After the addition of guanosine-5′-monophosphate (5′-GMP, 3 mM) as a model of DNA base, a peak of adduct for CDDP with 5′-GMP (platinated GMP) is observed along with the decrease in peak for complex **7** (Figures S9−S11), indicating its competence to cause DNA injury. Then, the stability and reduction rate of dual KP platinum(IV) complex **1** in the absence and presence of AsA in RPMI1640 were evaluated to compare with compound **7** (Figure S11a). Interestingly, mono-KP complex **7** possesses superior stability to dual KP complex **1** in RPMI1640. Meanwhile, hybrid **7** undergoes faster reduction in a reducing environment (AsA, 1 mM) than compound **1**.

Accordingly, these facts mentioned above might be the reason accounting for the distinct antitumor competence of complexes **1** and **7** in vitro and in vivo. The higher Log $P_{o/w}$

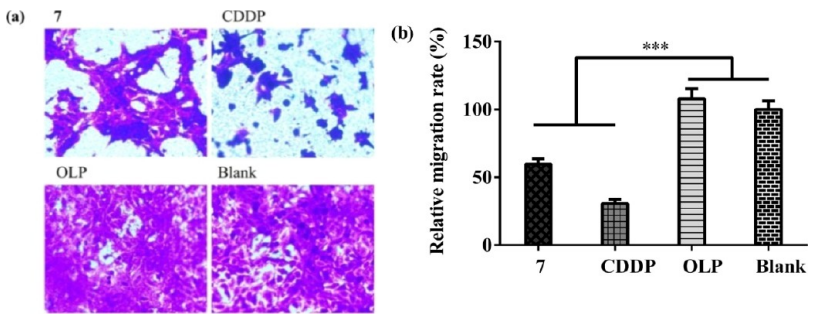

Figure 7. Evaluation of migration inhibition properties of complex 7, CDDP, and OLP (10 μM) to 4T1 cells using transwell assay in vitro. The tumor cells were treated with and without platinum complexes for 24 h. (a) Representative images. (b) Analysis of relative migration rate. *P < 0.05, **P < 0.01, ***P < 0.001, and *ns*: no significant difference.

https://doi.org/10.1021/acs.jmedchem.1c01236
J. Med. Chem. 2021, 64, 17920−17935

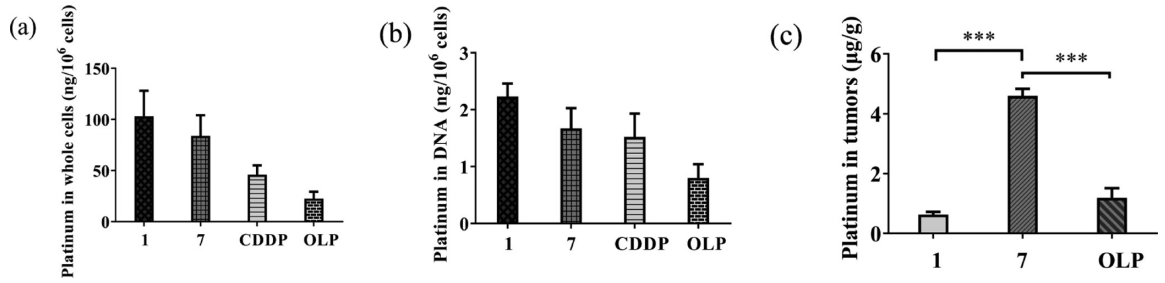

Figure 8. Drug accumulations in CT-26 cells and in DNA after treatment with platinum complexes (10 μM) for 24 h in vitro and in CT-26 tumor tissues in vivo. (a) Platinum in whole cells. (b) Platinum in DNA. (c) Platinum in tumors tissues. *P < 0.05, **P < 0.01, ***P < 0.001, and *ns*: no significant difference.

increases the cellular accumulation of complex **1** in vitro and results in the lower IC_{50} values than complex **7**. However, the poor stability of complex **1** in normal biological media blocks its transportation in body, decreases its accumulation in tumor tissue, and restrains the antitumor efficacy in vivo. In contrast, the better stability of complex **7** in normal tissues makes it more promising to reach the tumor cite and significantly increases its uptake in tumor tissues. Then, it undergoes easier reduction in TME and finally leads to better antitumor activities in vivo.

Phosphorylated H2AX (γ-H2AX) is a sensitive detectable marker for DNA double-strand breaks (DSBs). The growth-suppressor gene product p53 is another protein in response to Pt-DNA lesions, which is also tightly associated with the mitochondrial injury and ROS production. In addition, the lack of p53 function is an important factor in causing resistance of platinum(II) drugs in tumor cells.[48] Herein, the expression of γ-H2AX and p53 was evaluated by western blotting (Figure 9) to further evidence the DNA damage caused by complex **7**. Increased levels of γ-H2AX and p53 are observed in the complex **7**-treated group in contrast to the blank, which are even higher than reference drug CDDP, indicating the serious DNA damage caused by complex **7**. Moreover, the improved expression of p53 would exert much positive influence on overcoming of drug resistance. These facts reflect that the antitumor function for complex **7** is tightly related to the formation of DNA lesion in tumor cells.

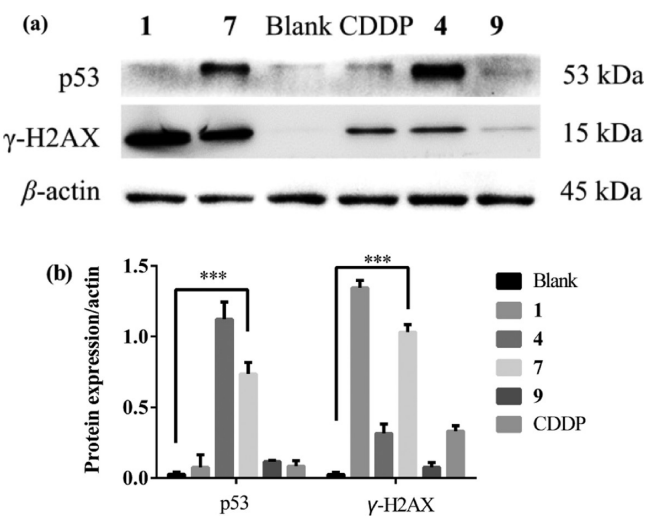

Figure 9. Western blot analysis of γ-H2AX and p53 expression. A549 cells were incubated with and without platinum compounds **1**, **4**, **7**, and **9** and CDDP (10 μM) for 24 h at 37 °C. (a) Blots. (b) Relative gray intensity analysis [relative gray intensity = (gray intensity of indicated protein)/(gray intensity of β-actin)]. *P < 0.05, **P < 0.01, ***P < 0.001, and *ns*: no significant difference.

Mitochondrial Apoptotic Pathway. Apoptosis is one of the major cell death profiles associated with multiple signaling pathways in tumor cells. To further determine the antitumor mechanisms of the title complexes, the apoptosis-inducing properties of complexes **1**, **4**, **7**, and **9** were detected in a murine tumor cell line 4T1 and a human tumor cell line A549, respectively, using an annexin V-FITC/propidium iodide (PI) double staining assay. The results in Figures 10 and S12 show that all tested platinum(IV) complexes exhibit effective apoptosis induction of both A549 and 4T1 cells after 24 h treatment. Especially, candidate complex **7** induces significant apoptosis of tumor cells in a dose-dependent manner.

In the intrinsic pathway, mitochondria as energy supply organelles display important roles in regulating apoptosis process. Platinum drugs could target mitochondria by inducing mitochondrial membrane depolarization ($\Delta\Psi_m$) and increasing ROS generation, which would be in favor of preventing drug resistance.[49] Additionally, the oxidizing potency of platinum(IV) complexes could promote ROS production, which would further drop $\Delta\Psi_m$ to induce mitochondria injury and leads to following downstream events in the apoptosis cascades. Thus, the $\Delta\Psi_m$ decrease in mitochondria and ROS generation in A549 and 4T1 cells were, respectively, detected using JC-1 and 2′,7′-dichlorofluorescein diacetate (DCFH-DA) staining assays. The tumor cells were incubated for 24 h at 37 °C with and without compounds **1**, **4**, **7**, and **9**, CDDP, CDDP + KP, and OLP. The ROS generation depicted in Figures S13 and S14 shows that platinum(IV) compounds **1**, **4**, **7**, and **9** lead to significantly high intracellular ROS levels in 4T1 and A549 cells in contrast to the untreated group, which are even higher than the platinum(II) drugs CDDP and OLP, as well as CDDP + KP. This trend is probably attributed to the oxidation function from platinum(IV) compounds besides the DNA damage. As for the competence in causing mitochondrial membrane depolarization (Figures 11 and S15), complexes **1**, **4**, **7**, and **9** also cause comparable or even more serious $\Delta\Psi_m$ loss than CDDP, OLP, and the mixture CDDP + KP. The trend of $\Delta\Psi_m$ loss is mainly in tune with the ROS production. It has been proven that the mitochondria damage would promote the expression of p53. The serious mitochondrial injuries caused by KP and LP platinum(IV) complexes are probably an inducement of high expression of p53, further accelerating apoptosis of tumor cells and preventing the development of drug resistance.

Then, the mitochondrial apoptotic proteins Bcl-2, Bax, caspase3, and *c*-caspase3 which were critical in the initiation

https://doi.org/10.1021/acs.jmedchem.1c01236
J. Med. Chem. 2021, 64, 17920−17935

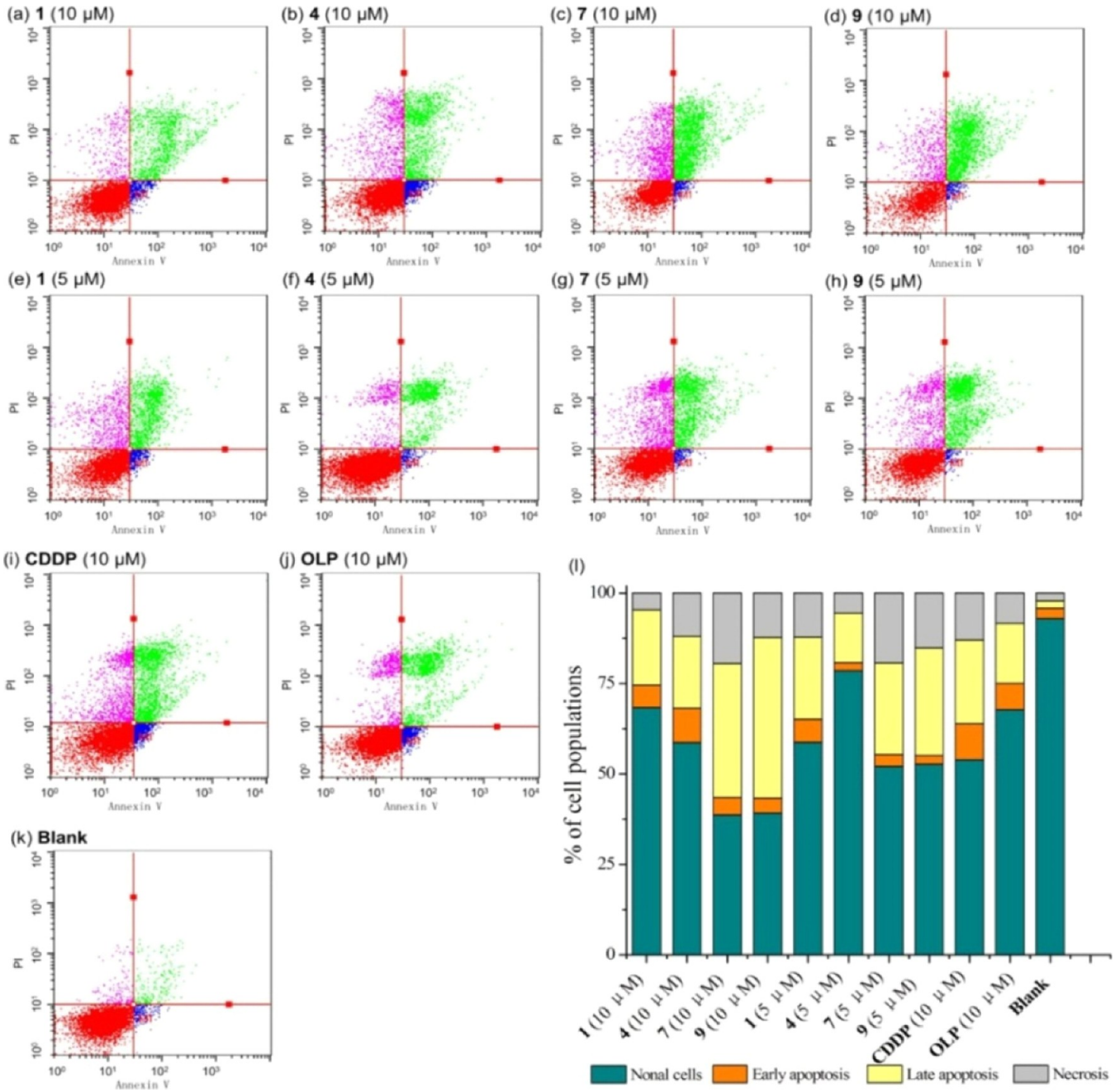

Figure 10. Quantification of apoptosis in A549 cells using an annexin V-FITC/PI staining assay. A549 cells were incubated with and without platinum complexes for 24 h at 37 °C. (a) **1** (10 μM). (b) **4** (10 μM). (c) **7** (10 μM). (d) **9** (10 μM). (e) **1** (5 μM). (f) **4** (5 μM). (g) **7** (5 μM). (h) **9** (5 μM). (i) CDDP (10 μM). (j) OLP (10 μM). (k) Blank. (l) Stacking columns.

and execution of apoptosis were testified. Blots in Figure 12 reveal that complexes **1**, **4**, **7**, and **9** are effective in modulating the expression of apoptotic proteins in tumor cells. The candidate complex **7** dramatically downregulates the level of anti-apoptotic Bcl-2 and increases the secretion of pro-apoptotic Bax. Subsequently, the apoptosis executor caspase3 and *c*-caspase3 are remarkably upregulated by compound **7**. It could be deduced that candidate complex **7** induces serious apoptosis of tumor cells by the activation of mitochondrial pathway Bcl-2/Bax/caspase3.

Inflammation Inhibition. Chronic inflammation as a hallmark of cancer plays a key role in promoting tumor proliferation, matrix degradation, and immunosuppression and is tightly associated with tumor occurrence, invasion, and metastasis. COX-2 and MMP-9 display multifaceted synergistic roles in promoting inflammation and metastasis in TME. Herein, the expression of COX-2 and MMP-9 in tumor cells in vitro and in tumor tissues in vivo were measured by western blot and immunohistochemistry.

Blots in Figure 13 demonstrate that COX-2 and MMP-9 expression in complex **7**-treated tumor cells are significantly reduced in contrast to the blank group in vitro ($P < 0.001$). Complex **1** with dual KP ligands possessing effective activities in vitro exerts even more potent COX-2 and MMP-9 inhibition than complex **7**, which is in tune with the antitumor activities in vitro. Then, immunohistochemical results of 4T1 tumor

https://doi.org/10.1021/acs.jmedchem.1c01236
J. Med. Chem. 2021, 64, 17920−17935

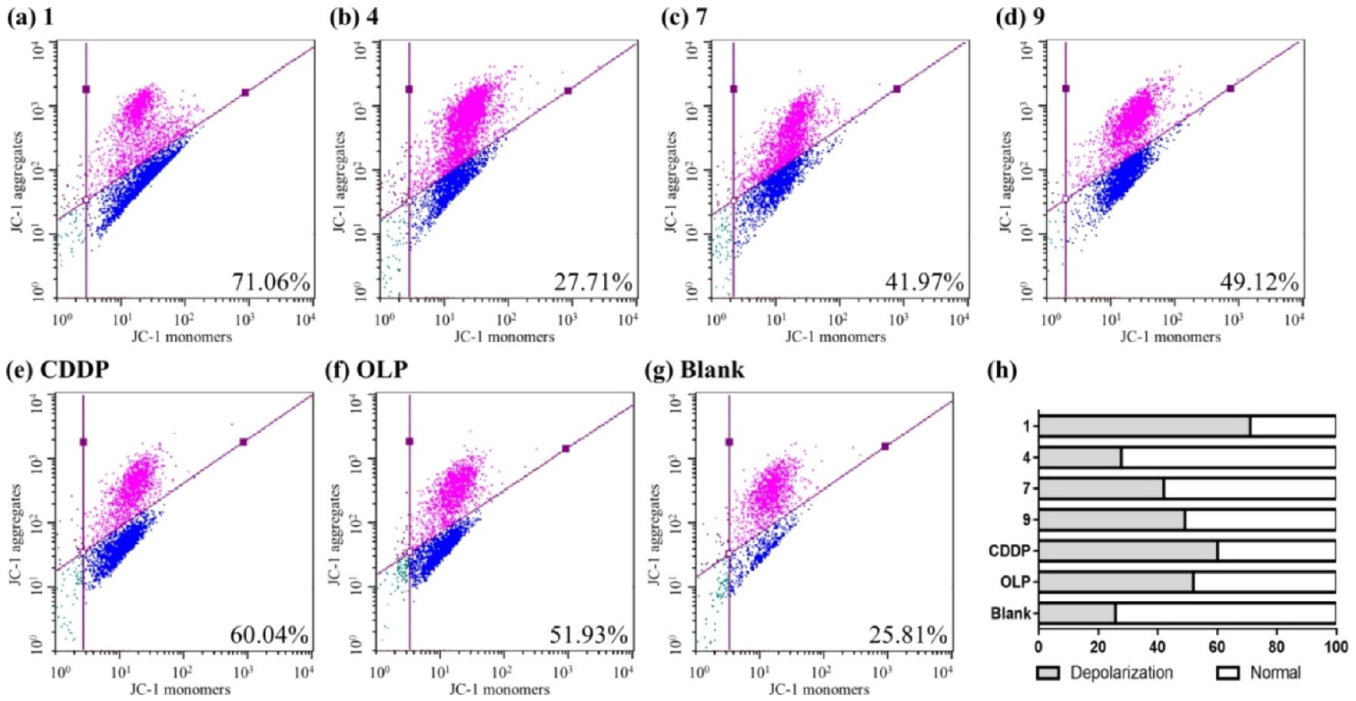

Figure 11. Mitochondrial membrane potential ($\Delta\Psi_m$) analyzed by flow cytometry. A549 cells were treated with and without platinum complexes (10 μM) for 24 h at 37 °C and stained with JC-1. (a) **1**. (b) **4**. (c) 7. (d) **9**. (e) CDDP. (f) OLP. (g) Blank. (h) Statistical analysis of the decrease in $\Delta\Psi_m$.

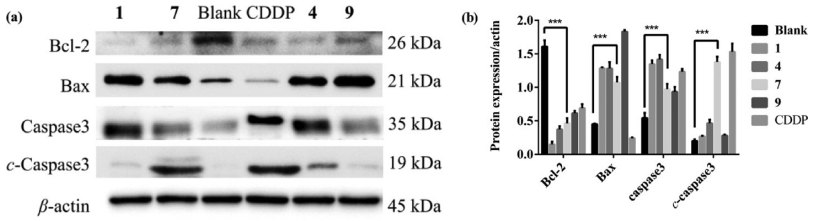

Figure 12. Western blot analysis of Bcl-2, Bax, caspase3, and *c*-caspase3 expression. A549 cells were incubated with and without platinum compounds **1**, **4**, 7, **9**, and CDDP (10 μM) for 24 h at 37 °C. (a) Blots. (b) Relative gray intensity analysis. *P < 0.05, **P < 0.01, ***P < 0.001, and *ns*: no significant difference.

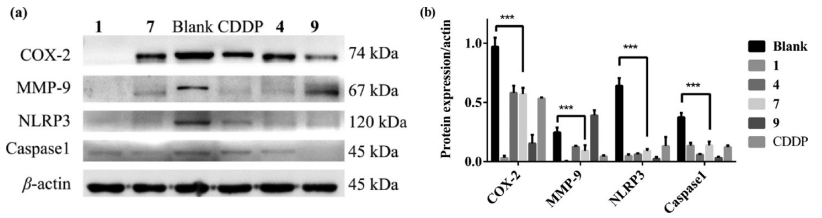

Figure 13. Western blot analysis of COX-2, MMP-9, NLRP3, and caspase1 in A549 cells treated by platinum complexes. A549 cells were incubated with and without compounds **1**, **4**, 7, and **9** and CDDP (10 μM) for 24 h at 37 °C. (a) Blots. (b) Relative gray intensity analysis. *P < 0.05, **P < 0.01, ***P < 0.001, and *ns*: no significant difference.

tissues in vivo (Figure 14) display that complex 7 decreases the expression of COX-2 and MMP-9 to 22.3 and 22.0% of the blank group (P < 0.001), which are significantly lower than CDDP (54.3 and 95.6%, P < 0.001). Moreover, the immunohistochemical results of CT-26 tumors (Figure S4) further evidence the inhibitory competence of complex 7 to COX-2 and MMP-9 that complex 7 inhibits the expression of COX-2 and MMP-9 to 10.5 and 27.7%, respectively, which is more effective than OLP (118.3 and 138.7%). Notably, the inhibitory competence of candidate 7 to COX-2 and MMP-9 in CT-26 tumors is even higher than complex **1** (21.5 and 48.2%), which are in accordance with their accumulation in tissues and antitumor activities in vivo. In view of this, although platinum(II) drugs CDDP and OLP effectively suppress the growth of tumors in vivo, they exert negligible effects on restraining inflammatory reaction in TME. In contrast, KP platinum(IV) 7 is effective in reducing inflammation both in vitro and in vivo besides the potent antitumor competence, which would be an important factor attributing for its potent antimetastasis properties.

NLRP3 inflammasome as a multiprotein complex responsible for the processing of caspase1 plays major roles in

https://doi.org/10.1021/acs.jmedchem.1c01236
J. Med. Chem. 2021, 64, 17920−17935

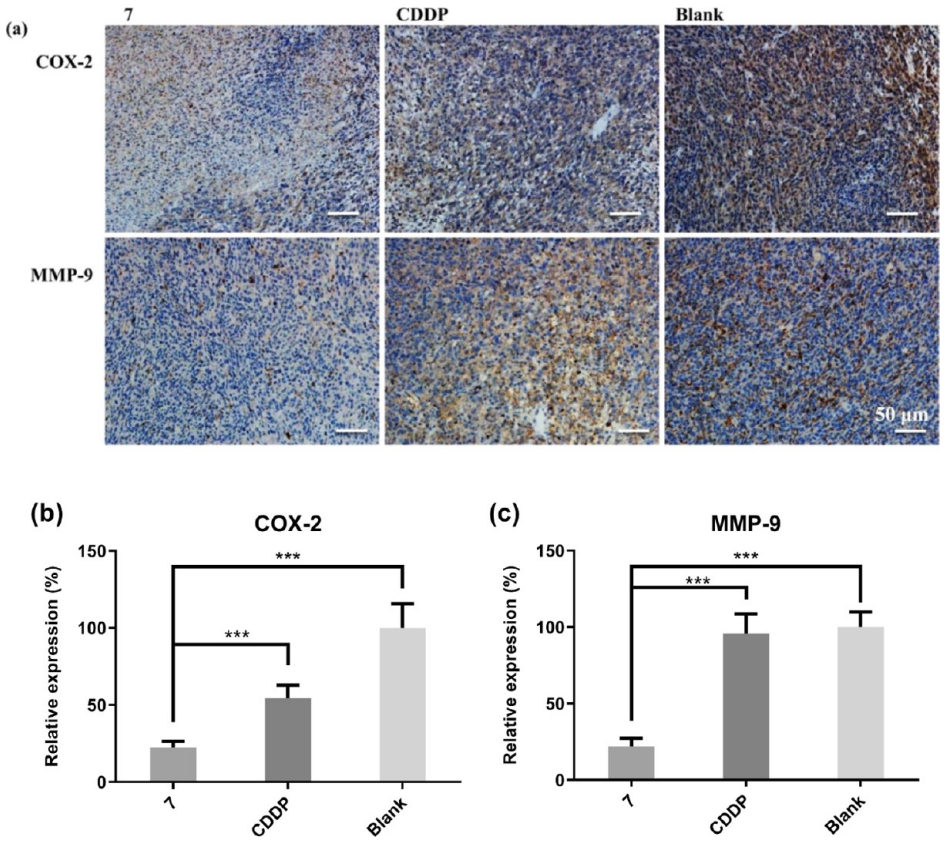

Figure 14. Immunohistochemical staining of COX-2 and MMP-9 in 4T1 tumors treated by complex **7**, CDDP, and saline. (a) Representative micrographs. (b) Analysis of COX-2 expression. (c) Analysis of MMP-9 expression. *P < 0.05, **P < 0.01, ***P < 0.001, and *ns*: no significant difference.

promoting inflammatory diseases. Recently, NLRP3 has been implicated in tumor development and dissemination.[50−52] The NSAIDs were repurposed as potent NLRP3 inflammasome inhibitors independently of COX enzymes in recent works.[53] Thus, the effects of the title KP and LP platinum(IV) complexes on NLRP3 and caspase1 expression in tumor cells were investigated. It is observed that NLRP3 and caspase1 are remarkably downregulated by complex **7** (Figure 13) indicating that the suppression of the NLRP3/caspase1 pathway is another route for complex **7** to inhibit tumor inflammation. Complexes **1**, **4**, and **9** also exhibit prominent inhibition to these two proteins. Accordingly, candidate complex **7** with effective antitumor activities in vitro and in vivo could suppress COX-2, MMP-9, NLRP3, and caspase1 simultaneously to alleviate the inflammation in TME and inhibit metastasis.

Immunity Activation. The suppressed immune responses in tumors play an essential role in promoting immune evasion and metastasis of tumor cells. PD-L1 as an immunosuppressive molecule highly expressed in various tumors could combine with PD-1 on the surface of T cells to drive T cell dysfunction and induce immunosuppression. Restraining inflammation in TME would reduce PD-L1 expression significantly. The blockade of PD-1−PD-L1 interaction triggers the activation of tumor-infiltrating lymphocytes (TILs) such as $CD3^+$, $CD4^+$, and $CD8^+$ T cells,[54] the density of which in tumor tissues correlates with smaller tumor size, reduced relapse rate, and improved overall survival.[55] Herein, PD-L1 expression in both 4T1 and CT-26 tumor tissues was examined by immunohistochemistry, and the $CD3^+$ and $CD8^+$ T cells were immunohistochemically stained. Results in Figure 15 depict that complex **7** dramatically suppresses the secretion PD-L1 in 4T1 tumors to 22.2% of the blank group (P < 0.001), which is significantly lower than its precursor CDDP (54.3%, P < 0.001). Subsequently, the density of $CD3^+$ and $CD8^+$ T cells is simultaneously increased by the complex **7** in 5.4- and 7.3-fold of the blank group (P < 0.001), indicating its prominent competence in arousing T cell immunity. Then, the expression of PD-L1 in CT-26 tumors (Figure S5) is also significantly inhibited by complex **7** to 13.2%, which is lower than OLP (149.62%) as well as dual KP complex **1** (29.3%). Then, significantly increasing amounts of $CD3^+$ and $CD8^+$ T cells are also observed in complex **7**-treated CT-26 tumors. Notably, platinum(II) drugs CDDP and OLP display negligible effects on $CD3^+$ and $CD8^+$ T cells in 4T1 and CT-26 tumor tissues, reflecting their negative competence in reversing immune suppression in these models. Collectively, KP platinum(IV) complex **7** exerts antitumor and antimetastasis activities by boosting immune functions in tumor tissues via restraining of PD-L1 expression and further increasing the density of $CD3^+$ and $CD8^+$ TILs.

CONCLUSIONS

Metastasis is the leading cause of mortality for patients suffering from cancer. Chronic inflammation and immune suppression in TME highly promotes the metastasis of tumor cells. Traditional platinum(II) drugs failed in treatment of metastatic cancers. In this work, a series of new platinum(IV) complexes bearing KP and LP ligands were designed and synthesized as antitumor agents by integrating chemotherapy

https://doi.org/10.1021/acs.jmedchem.1c01236
J. Med. Chem. 2021, 64, 17920−17935

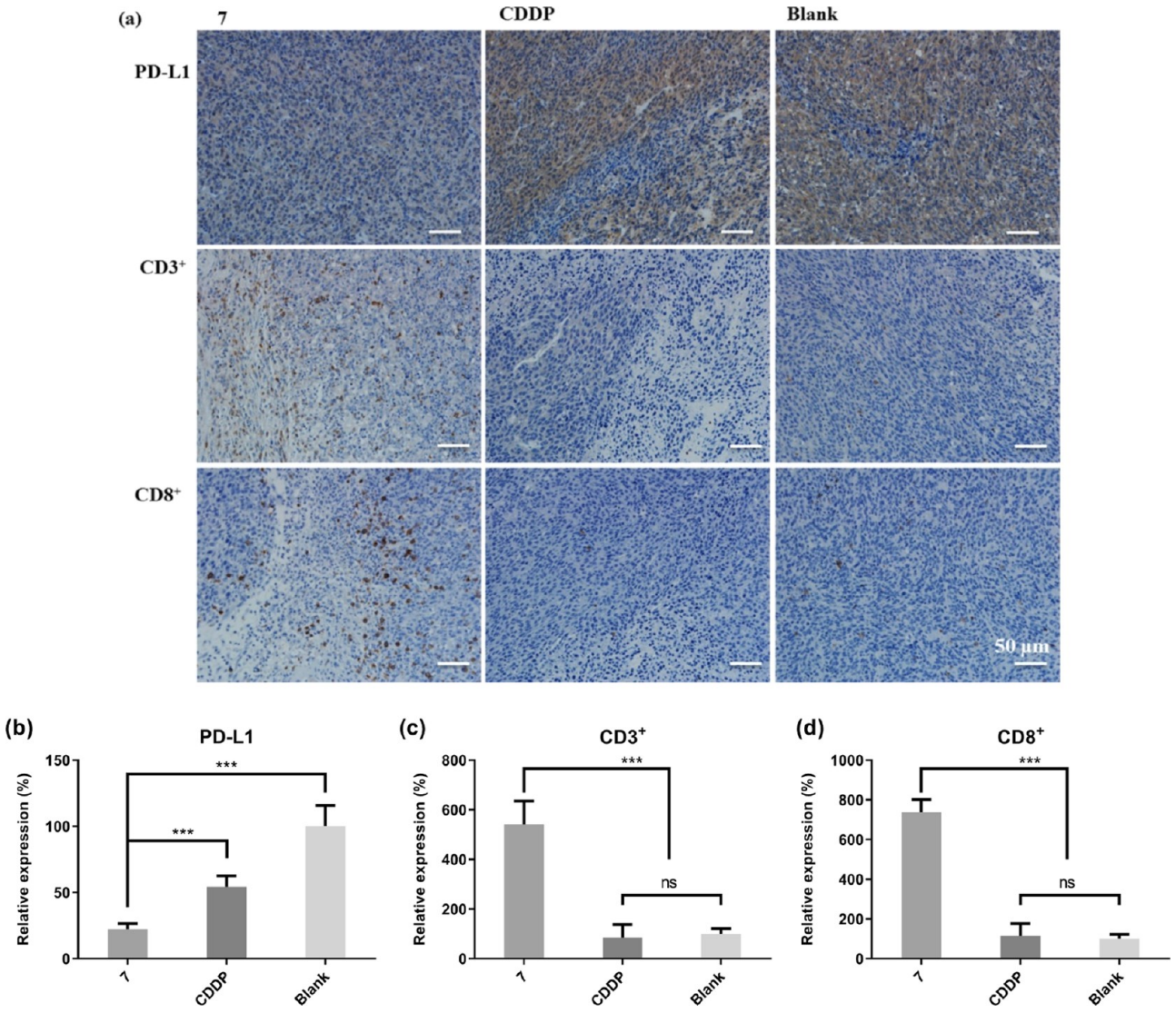

Figure 15. Immunohistochemical staining of PD-L1, $CD3^+$, and $CD8^+$ in 4T1 tumors treated by complex 7 and CDDP and saline. (a) Representative micrographs. (b) Quantified data of PD-L1 expression. (c) Quantified data of $CD3^+$ TILs. (d) Quantified data of $CD8^+$ TILs. $^*P < 0.05$, $^{**}P < 0.01$, $^{***}P < 0.001$, and *ns*: no significant difference.

and immunotherapy targeting COX-2, MMP-9, and PD-L1 besides DNA. Complex 7 possessing potent antitumor activities in vitro and in vivo is screened out as a candidate and exerts great potential in overcoming CDDP resistance (RF = 0.73) in contrast to CDDP (RF = 3.10). The TGI for complex 7 is as high as platinum(II) drugs against CT-26 (57.1%) and 4T1 tumors (54.6%); meanwhile, it induces lower toxicities in vivo. More importantly, complex 7 exerts remarkable antimetastatic activities against 4T1 tumors with an inhibition rate of 84.1% in vivo, which is significantly superior to that of CDDP (65.5%) and OLP (40.7%). Mechanism investigations reveal that prodrug 7 causes serious DNA damage after reduction to the divalent form and further upregulates the expression of γ-H2AX and p53. Then, ROS production and $\Delta\Psi_m$ decrease are induced accompanied with the initiation of the mitochondrial apoptotic pathway Bcl-2/Bax/caspase3. The increased ROS generation and γ-H2AX and p53 expression simultaneously facilitate compound 7 to overcome CDDP resistance. Furthermore, tumor-recruited inflammation in TME is attenuated by the suppression of key enzymes COX-2, MMP-9, NLRP3, and caspase1. Moreover, compound 7 reverses the negative immune regulation in tumor tissues by retarding the expression of PD-L1 and subsequently increases $CD3^+$ and $CD8^+$ T cells. In general, candidate complex 7 displays potent antiproliferative and antimetastatic activities by causing serious DNA damage, controlling inflammation, and enhancing immune response in TME simultaneously. Our study may provide a new strategy for the development of promising platinum(IV) complexes as antiproliferative and antimetastatic agents by integrating chemotherapy and immunotherapy.

EXPERIMENTAL SECTION

General. All reactions were carried out under an atmosphere of nitrogen in flame-dried glassware with magnetic stirring unless otherwise indicated. CDDP and OLP were purchased from Boyuan Pharmaceutical Co., Ltd (Jinan, China). Other reagents were purchased from Sigma, J&K, Aladdin, Innochem Company (Beijing, China). ^{1}H NMR and ^{13}C NMR spectra were recorded on a Bruker spectrometer (500 and 126 MHz). The NMR chemical shifts were referenced to residual solvent peaks or to TMS as an internal standard. All coupling constants J were quoted in Hz. The HPLC analyses were performed on a Thermo Ultimate 3000 RS equipped

https://doi.org/10.1021/acs.jmedchem.1c01236
J. Med. Chem. 2021, 64, 17920−17935

with an Agilent Eclipse XDB-C18 column (250 × 4.6 mm, 5 μm). Mass spectra (MS) were obtained on a Shimadzu LC−MS/MS 8040 mass spectrometer with ESI ionization. Flow cytometry was performed on a Millipore Guava easyCyte 8HT flow cytometer. All compounds are >95% pure by HPLC analysis.

In Vitro Cellular Cytotoxicity Assays. Platinum(IV) complexes **1**−**10** and reference drugs KP, LP, CDDP, OLP, and CBP, as well as the mixture of CDDP/OLP and KP with a molar ratio of 1:1 (CDDP/OLP + KP, 1:1), were evaluated for antitumor activities in vitro against six tumor cell lines including human ovarian cancer (SKOV-3), human lung cancer (A549), cisplatin-resistant human lung cancer (A549R), murine colon cancer (CT-26), human liver cancer (HepG-2), and murine breast cancer (4T1) using an MTT assay. Then, a human normal liver cell line LO2 was also evaluated to detect the toxicity of the tested compounds to normal cells. The RPMI1640 containing 10% FBS was applied as a culture medium for the cells. Cells were seeded in 96-well plates (5×10^3), preincubated for 12 h in a humidified atmosphere containing 5% CO_2 at 37 °C, and then treated with the tested complexes for 48 h. Then, 20 μL of freshly prepared MTT solution (5 mg/mL in PBS) was added and the cells were further incubated for another 4 h. After that, the culture medium was removed and the MTT formazan was dissolved in DMSO (150 μL). Absorbance was quantified using a microplate reader (570 nm). The IC_{50} values of platinum complexes **1** and **7**, CDDP, and OLP toward CT26 for 24, 48, and 72 h continuous treatment were evaluated to detect the suitable treatment period for antitumor evaluation, and 48 h continuous treatment was selected. The IC_{50} values were calculated based on three parallel experiments.

In Vivo Antitumor and Antimetastasis Assays. BALB/c mice were purchased from Pengyue Experimental Animal Company (Jinan, China). All mice had access to food and water ad libitum with a 12:12 h light cycle and were maintained under temperature control (23 ± 2 °C). This study was performed in strict accordance with the NIH guidelines for the care and use of laboratory animals (NIH Publications no. 8023, revised 1978) and was approved by the Institute Animal Ethics Committee of Liaocheng University.

The solid tumor study against CT-26 tumors was carried out on male BALB/c mice (18−20 g). Murine CT-26 cells (1×10^6) suspended in PBS (0.15 mL) were injected subcutaneously into the left flank of mice and therapy was started when the tumor nodules were palpable on day 3. Then, the mice were randomly divided into 7 groups (n = 6): blank (saline), **1**, **4**, **7**, and **9**, CDDP, and OLP groups. Drugs dissolved in saline were administered intraperitoneally (4 mg Pt kg^{-1}, i.p.) four times on days 3, 6, 9, and 12 post-tumor inoculation. The tumor volume (V) was monitored during the experiment as $V = L \times W^2/2$, where the length (L) and width (W) were measured. Then, mice were sacrificed on day 17, and the blood, tumors, and tissues including the liver, heart, spleen, lung, and kidney were collected. Weights of tumors were weighed and the tumor growth inhibition rate (TGI) was calculated as follows: TGI = (1 − tumor weight of the drug-treated group/tumor weight of the saline group) × 100%. The tumor and organs of each group were fixed in 4% formaldehyde overnight, paraffin-embedded, and cut with a microtome (5 μm sections). Then, the slices were stained by H&E.

To further verify the antitumor activities of complex **7** in vivo, its activities toward 4T1 tumors were carried out on female BALB/C mice (18−20 g). Murine 4T1 cells (1×10^6) suspended in PBS (0.15 mL) were injected subcutaneously into the left flank of BALB/c mice and therapy was started when the tumor nodules were palpable on day 3. Four groups including complex **7** (4 mg Pt kg^{-1}), OLP (4 mg Pt kg^{-1}), CDDP (2 mg Pt kg^{-1}), and blank (saline) were set (n = 5). Mice were administrated with different drugs (i.p.) on days 3, 6, 9, and 12 and euthanized on day 15. The data were collected and analyzed as mentioned above.

For the antimetastasis experiment, 4T1 cells (2×10^5) in 0.1 mL of PBS were injected via the tail vein to establish the pulmonary metastasis models. Four groups of mice were randomly divided (n = 5) and treated (i. p.) by complex **7** (2 mg Pt kg^{-1}), CDDP (2 mg Pt kg^{-1}), OLP (2 mg Pt kg^{-1}), and saline (blank group) seven times on days 2, 4, 6, 8, 10, 12, and 14. The mice were sacrificed on day 14 after the last administration, and the lungs were collected. Then, the pulmonary metastasis nodules of each mouse were counted and analyzed after fixation with Bouin's fluid for 24 h. Then, the lungs were paraffin-embedded, cut with a microtome (5 μm sections), and stained by H&E.

Wound-Healing Assay. The 4T1 cells (8×10^5) were seeded in a six-well cell-culture plate and incubated for 12 h at 37 °C until the cells grew to 90% confluency. Then, a wound was generated in each well. The cells were treated with complex **7**, CDDP, and OLP at 10 μM in RPMI1640 medium with 1% FBS, and the untreated well was set as the blank. The extent of wound healing was monitored at 0, 12, and 24 h. The wound-healing rate was calculated to assess the directional migration potency of the cells treated using different drugs in vitro.

Transwell Migration Assay. The transwell migration assay was conducted with a 24-well chamber (Costar 3422) containing inserts (8 μm pores). In the migration assay, cells in RPMI1640 medium (5×10^4 cells in 0.2 mL) were seeded in the upper compartment of the chamber and culture media (0.6 mL) with 10% FBS with and without compounds (**7**, CDDP, and OLP: 10 μM) were added to the lower compartment. The cells were incubated for 24 h at 37 °C in a humidified atmosphere of 5% CO_2. After that, the cells were fixed with 4% paraformaldehyde for 20 min and stained with 0.1% crystal violet for 20 min. The nonmigrating cells in the upper chamber were scraped away gently using a cotton swab. The migrated cells on the lower surface were photographed with an inverted microscope (Olympus) in five random visual fields and the migrated cells were measured using Image J.

HPLC Assay. The reduction potential of platinum(IV) complex **7** and the DNA-binding properties were determined by HPLC. The HPLC analysis was performed on a Thermo Ultimate 3000 RS equipped with an Agilent Eclipse XDB-C18 column (250 × 4.6 mm, 5 μm). The HPLC spectra were recorded using a diode array detector. The injection volume was 10 μL. The flow rate was 1.0 mL/min. Phase A was water with 0.1% TFA, and phase B was methanol. The flow rate was 1.0 mL/min. The HPLC program was as follows: 10% phase B (stationary from 0 to 5 min); 10 to 60% phase B (linear increase from 5 to 25 min); 60 to 90% phase B (linear increase from 25 to 26 min); and 90% phase B (stationary from 26 to 34 min).

Solutions of complexes **1** (1 mM) and **7** (1 mM) in PBS and RPMI1640 were monitored for 24 h to investigate their stability. Then, solutions of complexes **1** (1 mM) and **7** (1 mM) in PBS and RPMI1640 containing AsA (1 mM, similar concentration as in TME) were measured to investigate their reduction potential under the reducing condition. 5′-GMP was used as a model of the DNA base. The PBS and RPMI1640 solutions containing complex **7** (1 mM), 5′-GMP (3 mM), and AsA (1 mM) were recorded by HPLC to demonstrate its DNA-binding properties. The DNA interaction competence was evidenced by the formation of the platinated GMP adduct (Pt-GMP) in Figures S9 and S11, which was verified by LCMS (Figure S10).

Determination of the Water−Octanol Partition Coefficient. Water−octanol partition coefficient (Log $P_{o/w}$) values of the platinum(IV) complexes **1** and **7** were tested by the shake flask method. Briefly, n-octanol used in the experiment was presaturated with ultrapure water containing 0.9% NaCl (w/v) overnight.[56] An n-octanol solution of platinum(IV) complex (1 mM) was added to an equal volume of ultrapure water with 0.9% NaCl (w/v), and the mixture was shaking for 30 min vigorously. After that, the mixture was centrifuged at 2000 rpm for 15 min to achieve phase separation. The amount of the complex in n-octanol and water phases was determined by HPLC. The results were obtained based on three parallel experiments. The Log $P_{o/w}$ values of CDDP and OLP were obtained from the literature.[45]

Apoptosis Experiment—Annexin V-FITC/PI Assay. The experiment was performed according to the manufacturer's protocol (Annexin V-FITC/PI Apoptosis Detection Kit, Beyotime Biotechnology, China).[57,58] Briefly, A549/4T1 cells (2×10^5) were preincubated in a six-well cell-culture plate for 12 h and treated with or without the tested compounds at 37 °C for 24 h. After that, cells were harvested

https://doi.org/10.1021/acs.jmedchem.1c01236
J. Med. Chem. 2021, 64, 17920−17935

and stained by annexin V-FITC and PI. Then, samples were immediately analyzed by flow cytometric assay.

Mitochondrial Membrane Potential Experiment—JC-1 Assay. A JC-1 assay was used to detect the mitochondrial membrane depolarization ($\Delta\Psi_m$) in tumor cells using a mitochondrial membrane potential assay kit (Solarbio, China). Briefly, A549/4T1 cells (2×10^5) were incubated in a six-well cell-culture plate for 12 h and treated with and without tested platinum complexes at a concentration of 10 μM for 24 h in an incubator at 37 °C. Then, cells were collected, stained by JC-1, and tested using a flow cytometric assay.

ROS Experiment—DCFH-DA Assay. The ROS production in tumor cells was detected using DCFH-DA using a fluorescence microscope and flow cytometric assays based on the ROS-dependent oxidation of DCFH to DCF.

For fluorescence microscope assay, A549 cells (2×10^5) were incubated in a six-well cell-culture plate for 12 h and treated with and without tested complexes for 24 h in an incubator at 37 °C. Then, cells were stained with DCFH-DA (10 μM) in free culture medium for 20 min and gently washed with cold PBS twice. Then, the cells were imaged with a fluorescence microscope (Olympus IX73) under visible light and blue light, respectively.

For flow cytometric assay, the A549/4T1 cells were treated with the tested complexes in procedures as mentioned above. Then, the cells were harvested, washed with PBS, and stained by DCFH-DA (10 μM) for 20 min. After that, the cells were washed with PBS three times and tested immediately by flow cytometry.

Western Blot Assay. The expression of γ-H2AX, p53, Bcl-2, Bax, caspase3, *c*-caspase3, COX-2, MMP-9, NLRP3, and caspase1 was evaluated by western blot assay. Briefly, A549 cells were exposed to drugs (blank: untreated group; compounds **1**, **4**, **7**, and **9** and CDDP: 10 μM) for 24 h at 37 °C and harvested. The proteins were isolated with lysis buffer and measured using a BCA protein assay kit (Sangon Biotec, China). The proteins (30 μg per Lane) were separated by 10% sodium dodecyl sulfate−polyacrylamide gel electrophoresis (Sangon Biotec, China) and transferred onto a polyvinylidene difluoride Immobilon-P membrane (Millipore). Then, the blots were blocked for 1 h using 5% nonfat milk in TBST (Tris-buffered saline plus 0.1% Tween 20). The membrane was incubated with primary antibodies γ-H2AX (Ser139) (Cell signaling Technology, U.S.A.), p53 (SANTA CRUZ Biotechnology, U.S.A.), Bcl-2 (ProteinTech, China), Bax (Servicebio, China), caspase3 (ProteinTech, China), *c*-caspase3 (Abcam, England), COX-2 (Abcam, England), MMP-9 (ProteinTech, China), NLRP3 (ABclonal Technolog, China), and caspase1 (ABclonal Technolog, China) overnight at 4 °C, washed with TBST (5 min) three times, incubated with a secondary antibody for 1 h at 37 °C, and washed with TBST (5 min) three times. Finally, the membrane was treated with an ECL western blotting substrate kit (ProteinTech, China) and imaged using a scanning system (Tanon 46000SF).

Immunohistochemical Assay. The expression of proteins COX-2, MMP-9, PD-L1, $CD3^+$, and $CD8^+$ in both 4T1 and CT-26 tumor tissues was tested by immunohistochemical assay. The formalin-fixed, paraffin-embedded tumor tissues were cut with a microtome (5 μm sections), deparaffinized, and hydrated. After that, the sections were boiled in citrate buffer under a microwave for antigen repair and further blocked for 60 min in 10% normal goat serum (Sigma, USA). Subsequently, the sections were incubated with primary antibody COX-2 (Servicebio, China), MMP-9 (Servicebio, China), PD-L1 (Servicebio, China), $CD3^+$ (Servicebio, China), and $CD8^+$ (Servicebio, China) overnight at 4 °C. Then, sections were incubated with goat antimouse IgE-HRP secondary antibody (Servicebio, China) for 50 min at room temperature. The sections were then visualized with 3,3′-diaminobenzidine (DAB) (Servicebio, China) and counterstained using hematoxylin. The slices were imaged using an inverted microscope (Olympus) for five random fields, and the expression of protein was measured using ImageJ.

■ ASSOCIATED CONTENT

Supporting Information

The Supporting Information is available free of charge at https://pubs.acs.org/doi/10.1021/acs.jmedchem.1c01236.

Synthesis of platinum(IV) complexes **1**−**10**, antitumor activities in vitro and in vivo, compound Log $P_{o/w}$, reduction and DNA damage properties, mitochondrial apoptotic pathway, and ^{1}H NMR, ^{13}C NMR, MS, and HPLC spectra (PDF)

Molecular formula strings (CSV)

■ AUTHOR INFORMATION

Corresponding Authors

Qingpeng Wang − *Institute of Biopharmaceutical Research, Liaocheng University, Liaocheng 252059, P. R. China; Liaocheng High-Tech Biotechnology Co., Limited, Liaocheng 252059, P. R. China;* orcid.org/0000-0002-2093-8237; Email: lywqp@126.com

Ning Zhang − *Institute of Biopharmaceutical Research, Liaocheng University, Liaocheng 252059, P. R. China;* orcid.org/0000-0003-2102-8611; Email: zhangning1111@126.com

Zhifang Liu − *Institute of Biopharmaceutical Research, Liaocheng University, Liaocheng 252059, P. R. China;* Email: lzflcu@126.com

Authors

Zuojie Li − *Institute of Biopharmaceutical Research, Liaocheng University, Liaocheng 252059, P. R. China*

Linming Li − *Institute of Biopharmaceutical Research, Liaocheng University, Liaocheng 252059, P. R. China*

Yan Chen − *Institute of Biopharmaceutical Research, Liaocheng University, Liaocheng 252059, P. R. China*

Jichun Cui − *Shandong Provincial Key Laboratory of Chemical Energy Storage and Novel Cell Technology, School of Chemistry and Chemical Engineering, Liaocheng University, Liaocheng 252059, P. R. China*

Min Liu − *Institute of Biopharmaceutical Research, Liaocheng University, Liaocheng 252059, P. R. China;* orcid.org/0000-0002-1918-9072

Jun Han − *Institute of Biopharmaceutical Research, Liaocheng University, Liaocheng 252059, P. R. China; Liaocheng High-Tech Biotechnology Co., Limited, Liaocheng 252059, P. R. China*

Zhengping Wang − *Institute of Biopharmaceutical Research, Liaocheng University, Liaocheng 252059, P. R. China; Liaocheng High-Tech Biotechnology Co., Limited, Liaocheng 252059, P. R. China*

Complete contact information is available at: https://pubs.acs.org/10.1021/acs.jmedchem.1c01236

Notes

The authors declare no competing financial interest.

■ ACKNOWLEDGMENTS

This work was supported by the National Natural Science Foundation of China (no. 21807056), the Natural Science Foundation of Shandong (no. ZR2017BH092), and Taishan Scholar Research Foundation. This work was also technically supported by Shandong Collaborative Innovation Center for Antibody Drugs and Engineering Research Center for Nanomedicine and Drug-Delivery Systems.

■ ABBREVIATIONS

AsA, ascorbic acid; CBP, carboplatin; CDDP, cisplatin; COX, cyclooxygenase; DMF, *N*,*N*-dimethylformamide; DMSO, dimethyl sulfoxide; 5′-GMP, guanosine-5′-monophosphate; HPLC, high-performance liquid chromatography; IC_{50}, half-maximal inhibitory concentration; ICP−MS, inductively coupled plasma−mass spectrometry; MTT, (3-(4,5-dimethylthiazol-2-yl))-2,5-diphenyltetrazolium bromide; RF, resistant factor; TBTU, *N*,*N*,*N*′,*N*′-tetramethyl-*O*-(benzotriazol-1-yl)uronium tetrafluoroborate; TEA, *N*,*N*,*N*-triethylamine; TGI, tumor growth inhibition; MMP, matrix metalloproteinase; OLP, oxaliplatin; PD-L1, programmed death ligand 1; ROS, reactive oxygen species; TME, tumor microenvironment

■ REFERENCES

(1) Bray, F.; Ferlay, J.; Soerjomataram, I.; Siegel, R. L.; Torre, L. A.; Jemal, A. Global cancer statistics 2018: globocan estimates of incidence and mortality worldwide for 36 cancers in 185 countries. *Ca-Cancer J. Clin.* **2018**, *68*, 394−424.

(2) Ferlay, J.; Colombet, M.; Soerjomataram, I.; Mathers, C.; Parkin, D. M.; Piñeros, M.; Znaor, A.; Bray, F. Estimating the global cancer incidence and mortality in 2018: globocan sources and methods. *Int. J. Cancer* **2019**, *144*, 1941−1953.

(3) Sonnenschein, C.; Soto, A. M. Cancer metastases: so close and so far. *J. Natl. Cancer Inst.* **2015**, *107*, djv236.

(4) Allardyce, C. S.; Dyson, P. J. Metal-based drugs that break the rules. *Dalton Trans.* **2016**, *45*, 3201−3209.

(5) Wong, E.; Giandomenico, C. M. Current status of platinum-based antitumor drugs. *Chem. Rev.* **1999**, *99*, 2451−2466.

(6) Gersten, B. K.; Fitzgerald, T. S.; Fernandez, K. A.; Cunningham, L. L. Ototoxicity and platinum uptake following cyclic administration of platinum-based chemotherapeutic agents. *J. Assoc. Res. Otolaryngol.* **2020**, *21*, 303−321.

(7) Jia, C.; Deacon, G. B.; Zhang, Y.; Gao, C. Platinum(IV) antitumor complexes and their nano-drug delivery. *Coord. Chem. Rev.* **2021**, *429*, 213640.

(8) Kenny, R. G.; Marmion, C. J. Toward multi-targeted platinum and ruthenium drugs-a new paradigm in cancer drug treatment regimens? *Chem. Rev.* **2019**, *119*, 1058−1137.

(9) Ravera, M.; Gabano, E.; McGlinchey, M. J.; Osella, D. A view on multi-action Pt(IV) antitumor prodrugs. *Inorg. Chim. Acta* **2019**, *492*, 32−47.

(10) Johnstone, T. C.; Suntharalingam, K.; Lippard, S. J. The next generation of platinum drugs: targeted Pt(II) agents, nanoparticle delivery, and Pt(IV) prodrugs. *Chem. Rev.* **2016**, *116*, 3436−3486.

(11) Tan, X.; Li, G.; Wang, Q.; Wang, B.; Li, D.; Wang, P. G. Small molecular platinum(IV) compounds as antitumor agents. *Prog. Chem.* **2018**, *30*, 831−846.

(12) Hanahan, D.; Weinberg, R. A. Hallmarks of cancer: the next generation. *Cell* **2011**, *144*, 646−674.

(13) Leon-Cabrera, S.; Schwertfeger, K. L.; Terrazas, L. I. Inflammation as a target in cancer therapy. *Mediators Inflammation* **2019**, *2019*, 1971698.

(14) Murata, M. Inflammation and cancer. *Environ. Health Prev. Med.* **2018**, *23*, 50.

(15) Harris, R. E.; Casto, B. C.; Harris, Z. M. Cyclooxygenase-2 and the inflammogenesis of breast cancer. *World J. Clin. Oncol.* **2014**, *5*, 677−692.

(16) Annabi, B.; Lord-Dufour, S.; Vézina, A.; Béliveau, R. Resveratrol targeting of carcinogen-induced brain endothelial cell inflammation biomarkers MMP-9 and COX-2 is sirt1-independent. *Drug Target Insights* **2012**, *6*, 1−11.

(17) Zhang, Z.; Chen, F.; Shang, L. Advances in antitumor effects of NSAIDs. *Cancer Manage. Res.* **2018**, *10*, 4631−4640.

(18) Zitvogel, L.; Tesniere, A.; Kroemer, G. Cancer despite immunosurveillance: immunoselection and immunosubversion. *Nat. Rev. Immunol.* **2006**, *6*, 715−727.

(19) Wang, X.; He, Q.; Shen, H.; Xia, A.; Tian, W.; Yu, W.; Sun, B. TOX promotes the exhaustion of antitumor $CD8^+$ T cells by preventing PD1 degradation in hepatocellular carcinoma. *J. Hepatol.* **2019**, *71*, 731−741.

(20) Thommen, D. S.; Schumacher, T. N. T cell dysfunction in cancer. *Cancer Cell* **2018**, *33*, 547−562.

(21) Wang, X.; Sun, Q.; Liu, Q.; Wang, C.; Yao, R.; Wang, Y. CTC immune escape mediated by PD-L1. *Med. Hypotheses* **2016**, *93*, 138−139.

(22) Prima, V.; Kaliberova, L. N.; Kaliberov, S.; Curiel, D. T.; Kusmartsev, S. COX2/mPGES1/PGE2 pathway regulates PD-L1 expression in tumor-associated macrophages and myeloid-derived suppressor cells. *Proc. Natl. Acad. Sci. U.S.A.* **2017**, *114*, 1117−1122.

(23) Botti, G.; Fratangelo, F.; Cerrone, M.; Liguori, G.; Cantile, M.; Anniciello, A. M.; Scala, S.; D'Alterio, C.; Trimarco, C.; Ianaro, A.; Cirino, G.; Caracò, C.; Colombino, M.; Palmieri, G.; Pepe, S.; Ascierto, P. A.; Sabbatino, F.; Scognamiglio, G. COX-2 expression positively correlates with PD-L1 expression in human melanoma cells. *J. Transl. Med.* **2017**, *15*, 46.

(24) Spector, D.; Krasnovskaya, O.; Pavlov, K.; Erofeev, A.; Gorelkin, P.; Beloglazkina, E.; Majouga, A. Pt(IV) prodrugs with NSAIDs as axial ligands. *Int. J. Mol. Sci.* **2021**, *22*, 3817.

(25) Chen, Y.; Wang, Q.; Li, Z.; Liu, Z.; Zhao, Y.; Zhang, J.; Liu, M.; Wang, Z.; Li, D.; Han, J. Naproxen platinum(IV) hybrids inhibiting cycloxygenases and matrix metalloproteinases and causing DNA damage: synthesis and biological evaluation as antitumor agents in vitro and in vivo. *Dalton Trans.* **2020**, *49*, 5192−5204.

(26) Zanellato, I.; Bonarrigo, I.; Ravera, M.; Gabano, E.; Gust, R.; Osella, D. The hexacarbonyldicobalt derivative of aspirin acts as a CO-releasing NSAID on malignant mesothelioma cells. *Metallomics* **2013**, *5*, 1604−1613.

(27) Jin, S.; Muhammad, N.; Sun, Y.; Tan, Y.; Yuan, H.; Song, D.; Guo, Z.; Wang, X. Multispecific platinum(IV) complex deters breast cancer via interposing inflammation and immunosuppression as an inhibitor of COX-2 and PD-L1. *Angew. Chem., Int. Ed. Engl.* **2020**, *59*, 23313−23321.

(28) Song, X.-Q.; Ma, Z.-Y.; Wu, Y.-G.; Dai, M.-L.; Wang, D.-B.; Xu, J.-Y.; Liu, Y. New NSAID-Pt(IV) prodrugs to suppress metastasis and invasion of tumor cells and enhance anti-tumor effect in vitro and in vivo. *Eur. J. Med. Chem.* **2019**, *167*, 377−387.

(29) Neumann, W.; Crews, B. C.; Marnett, L. J.; Hey-Hawkins, E. Conjugates of cisplatin and cyclooxygenase inhibitors as potent antitumor agents overcoming cisplatin resistance. *ChemMedChem* **2014**, *9*, 1150−1153.

(30) Tolan, D. A.; Abdel-Monem, Y. K.; El-Nagar, M. A. Anti-tumor platinum (IV) complexes bearing the anti-inflammatory drug naproxen in the axial position. *Appl. Organomet. Chem.* **2019**, *33*, No. e4763.

(31) Tan, J.; Li, C.; Wang, Q.; Li, S.; Chen, S.; Zhang, J.; Wang, P. C.; Ren, L.; Liang, X.-J. A carrier-free nanostructure based on platinum(IV) prodrug enhances cellular uptake and cytotoxicity. *Mol. Pharm.* **2018**, *15*, 1724−1728.

(32) Dhar, S.; Pathak, R. Combined chemo-anti-inflammatory prodrugs and nanoparticles. *Synlett* **2016**, *27*, 1607−1612.

(33) Curci, A.; Denora, N.; Iacobazzi, R. M.; Ditaranto, N.; Hoeschele, J. D.; Margiotta, N.; Natile, G. Synthesis, characterization and in vitro cytotoxicity of a kiteplatin-ibuprofen Pt(IV) prodrug. *Inorg. Chim. Acta* **2018**, *472*, 221−228.

(34) Cheng, Q.; Shi, H.; Wang, H.; Wang, J.; Liu, Y. Asplatin enhances drug efficacy by altering the cellular response. *Metallomics* **2016**, *8*, 672−678.

(35) Kamei, S.; Sakayama, K.; Tamashiro, S.; Aizawa, J.; Miyawaki, J.; Miyazaki, T.; Yamamoto, H.; Norimatsu, Y.; Masuno, H. Ketoprofen in topical formulation decreases the matrix metalloproteinase-2 expression and pulmonary metastatic incidence in nude mice with osteosarcoma. *J. Orthop. Res.* **2009**, *27*, 909−915.

(36) Sakayama, K.; Kidani, T.; Miyazaki, T.; Shirakata, H.; Kimura, Y.; Kamogawa, J.; Masuno, H.; Yamamoto, H. Effect of ketoprofen in topical formulation on vascular endothelial growth factor expression

https://doi.org/10.1021/acs.jmedchem.1c01236
J. Med. Chem. 2021, 64, 17920−17935

and tumor growth in nude mice with osteosarcoma. *J. Orthop. Res.* **2004**, *22*, 1168−1174.
(37) Kanda, A.; Ebihara, S.; Takahashi, H.; Sasaki, H. Loxoprofen sodium suppresses mouse tumor growth by inhibiting vascular endothelial growth factor. *Acta Oncol.* **2003**, *42*, 62−70.
(38) Ravera, M.; Zanellato, I.; Gabano, E.; Perin, E.; Rangone, B.; Coppola, M.; Osella, D. Antiproliferative activity of Pt(IV) conjugates containing the non-steroidal anti-inflammatory drugs (NSAIDs) ketoprofen and naproxen. *Int. J. Mol. Sci.* **2019**, *20*, 3074.
(39) Ma, Z.-Y.; Song, X.-Q.; Hu, J.-J.; Wang, D.-B.; Ding, X.-J.; Liu, R.-P.; Dai, M.-L.; Meng, F.-Y.; Xu, J.-Y. Ketoplatin in triple-negative breast cancer cells MDA-MB-231: High effcacy and low toxicity, and positive impact on inflammatory microenvironment. *Biochem. Pharmacol.* **2021**, *188*, 114523.
(40) Ma, J.; Wang, Q.; Huang, Z.; Yang, X.; Nie, Q.; Hao, W.; Wang, P. G.; Wang, X. Glycosylated platinum(IV) complexes as substrates for glucose transporters (GLUTs) and organic cation transporters (OCTs) exhibited cancer targeting and human serum albumin binding properties for drug delivery. *J. Med. Chem.* **2017**, *60*, 5736−5748.
(41) Wang, Q.; Huang, Z.; Ma, J.; Lu, X.; Zhang, L.; Wang, X.; George Wang, P. Design, synthesis and biological evaluation of a novel series of glycosylated platinum(IV) complexes as antitumor agents. *Dalton Trans.* **2016**, *45*, 10366−10374.
(42) Liu, Z.; Li, Z.; Du, T.; Chen, Y.; Wang, Q.; Li, G.; Liu, M.; Zhang, N.; Li, D.; Han, J. Design, synthesis and biological evaluation of dihydro-2-quinolone platinum(IV) hybrids as antitumor agents displaying mitochondria injury and DNA damage mechanism. *Dalton Trans.* **2021**, *50*, 362−375.
(43) Cheng, Q.; Shi, H.; Wang, H.; Min, Y.; Wang, J.; Liu, Y. The ligation of aspirin to cisplatin demonstrates significant synergistic effects on tumor cells. *Chem. Commun.* **2014**, *50*, 7427−7430.
(44) Petruzzella, E.; Sirota, R.; Solazzo, I.; Gandin, V.; Gibson, D. Triple action Pt(IV) derivatives of cisplatin: a new class of potent anticancer agents that overcome resistance. *Chem. Sci.* **2018**, *9*, 4299−4307.
(45) Oldfield, S. P.; Hall, M. D.; Platts, J. A. Calculation of lipophilicity of a large, diverse dataset of anticancer platinum complexes and the relation to cellular uptake. *J. Med. Chem.* **2007**, *50*, 5227−5237.
(46) Karmakar, S.; Kostrhunova, H.; Ctvrtlikova, T.; Novohradsky, V.; Gibson, D.; Brabec, V. Platinum(IV)-estramustine multiaction prodrugs are effective antiproliferative agents against prostate cancer cells. *J. Med. Chem.* **2020**, *63*, 13861−13877.
(47) Liu, H.; Ma, J.; Li, Y.; Yue, K.; Li, L.; Xi, Z.; Zhang, X.; Liu, J.; Feng, K.; Ma, Q.; Liu, S.; Guo, S.; Wang, P. G.; Wang, C.; Xie, S. Polyamine-based Pt(IV) prodrugs as substrates for polyamine transporters preferentially accumulate in cancer metastases as DNA and polyamine metabolism dual-targeted antimetastatic agents. *J. Med. Chem.* **2019**, *62*, 11324−11334.
(48) Wang, D.; Lippard, S. J. Cellular processing of platinum anticancer drugs. *Nat. Rev. Drug Discovery* **2005**, *4*, 307−320.
(49) Cao, W.-q.; Zhai, X.-q.; Ma, J.-w.; Fu, X.-q.; Zhao, B.-s.; Zhang, P.; Fu, X.-y. Natural borneol sensitizes human glioma cells to cisplatin-induced apoptosis by triggering ROS-mediated oxidative damage and regulation of MAPKs and PI3K/AKT pathway. *Pharm. Biol.* **2020**, *58*, 72−79.
(50) Kolb, R.; Liu, G.-H.; Janowski, A. M.; Sutterwala, F. S.; Zhang, W. Inflammasomes in cancer: a double-edged sword. *Protein Cell* **2014**, *5*, 12−20.
(51) Wang, Y.; Kong, H.; Zeng, X.; Liu, W.; Wang, Z.; Yan, X.; Wang, H.; Xie, W. Activation of NLRP3 inflammasome enhances the proliferation and migration of A549 lung cancer cells. *Oncol. Rep.* **2016**, *35*, 2053−2064.
(52) Petrilli, V. The multifaceted roles of inflammasome proteins in cancer. *Curr. Opin. Oncol.* **2017**, *29*, 35−40.
(53) Daniels, M. J. D.; Rivers-Auty, J.; Schilling, T.; Spencer, N. G.; Watremez, W.; Fasolino, V.; Booth, S. J.; White, C. S.; Baldwin, A. G.; Freeman, S.; Wong, R.; Latta, C.; Yu, S.; Jackson, J.; Fischer, N.; Koziel, V.; Pillot, T.; Bagnall, J.; Allan, S. M.; Paszek, P.; Galea, J.; Harte, M. K.; Eder, C.; Lawrence, C. B.; Brough, D.; Brough, D. Fenamate NSAIDs inhibit the NLRP3 inflammasome and protect against alzheimer's disease in rodent models. *Nat. Commun.* **2016**, *7*, 12504.
(54) Xu-Monette, Z. Y.; Zhang, M.; Li, J.; Young, K. H. PD-1/PD-L1 Blockade: have we found the key to unleash the antitumor immune response? *Front. Immunol.* **2017**, *8*, 1597.
(55) Tan, Y.; Trent, J. C.; Wilky, B. A.; Kerr, D. A.; Rosenberg, A. E. Current status of immunotherapy for gastrointestinal stromal tumor. *Cancer Gene Ther.* **2017**, *24*, 130−133.
(56) Tabrizi, L.; Thompson, K.; Mnich, K.; Chintha, C.; Gorman, A. M.; Morrison, L.; Luessing, J.; Lowndes, N. F.; Dockery, P.; Samali, A.; Erxleben, A. Novel Pt(IV) pro-drugs displaying antimitochondrial effects. *Mol. Pharm.* **2020**, *17*, 3009−3023.
(57) Li, Z.; Chen, Y.; Liu, Z.; Wang, Q.; Zhao, Y.; Wei, J.; Liu, M.; Wang, Z.; Li, D.; Han, J. Synthesis and biological evaluation of new mono naphthalimide platinum(IV) derivatives as antitumor agents with dual DNA damage mechanism. *Monatsh. Chem.* **2020**, *151*, 353−367.
(58) Wang, Q.; Chen, Y.; Li, G.; Zhao, Y.; Liu, Z.; Zhang, R.; Liu, M.; Li, D.; Han, J. A potent aminonaphthalimide platinum(IV) complex with effective antitumor activities in vitro and in vivo displaying dual DNA damage effects on tumor cells. *Bioorg. Med. Chem. Lett.* **2019**, *29*, 126670.

https://doi.org/10.1021/acs.jmedchem.1c01236
J. Med. Chem. 2021, 64, 17920−17935